Journal Pre-proof

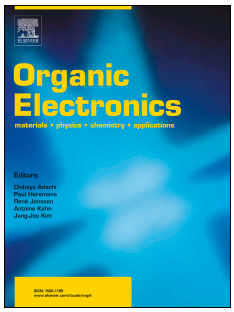

High-performance sky-blue phosphorescent organic light-emitting diodes employing wide-bandgap bipolar host materials with thermally activated delayed fluorescence characteristics

Yuan-Lan Zhang, Quan Ran, Qiang Wang, Qi-Sheng Tian, Fan-Cheng Kong, Jian Fan, Liang-Sheng Liao

PII: S1566-1199(20)30046-X

DOI: https://doi.org/10.1016/j.orgel.2020.105660

Reference: ORGELE 105660

To appear in: *Organic Electronics*

Received Date: 9 November 2019

Revised Date: 28 December 2019

Accepted Date: 20 January 2020

Please cite this article as: Y.-L. Zhang, Q. Ran, Q. Wang, Q.-S. Tian, F.-C. Kong, J. Fan, L.-S. Liao, High-performance sky-blue phosphorescent organic light-emitting diodes employing wide-bandgap bipolar host materials with thermally activated delayed fluorescence characteristics, *Organic Electronics* (2020), doi: https://doi.org/10.1016/j.orgel.2020.105660.

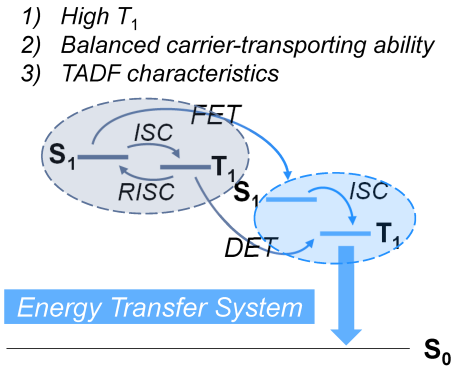

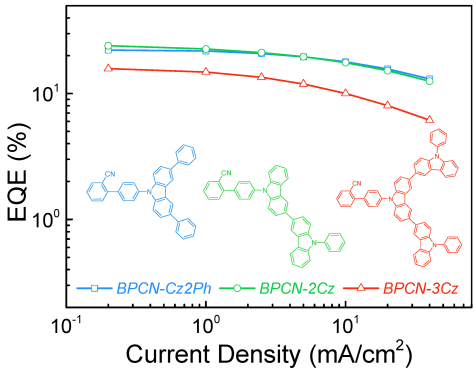

High-Performance Sky-Blue Phosphorescent Organic Light-Emitting Diodes Employing Wide-Bandgap Bipolar Host Materials with Thermally Activated Delayed Fluorescence Characteristics

Yuan-Lan Zhang,[1,†] Quan Ran,[1,†] Qiang Wang,[1] Qi-Sheng Tian,[1] Fan-Cheng Kong,[1] Jian Fan,[1,2,] and Liang-Sheng Liao[1,2,]**

[1]Institute of Functional Nano & Soft Materials (FUNSOM), Jiangsu Key Laboratory for Carbon-Based Functional Materials & Devices, Soochow University, Suzhou, Jiangsu 215123, P. R. China.

[2]Institute of Organic Optoelectronics, Jiangsu Industrial Technology Research Institute (JITRI), Wujiang, Suzhou, Jiangsu 215211, P. R. China.

E-mail: lsliao@suda.edu.cn; jianfan@suda.edu.cn

†These two authors contributed equally to this work.

Abstract: Up to date, several kinds of thermally activated delayed fluorescence (TADF) host molecules have been rapidly developed to fulfill the increasing demand of high-efficiency phosphorescent organic light-emitting diodes (PHOLEDs). Herein, three wide-bandgap TADF materials **BPCN-Cz2Ph**, **BPCN-2Cz**, and **BPCN-3Cz** are newly designed and synthesized as host materials for sky-blue PHOLEDs. By modulation of carbazole-units in the molecular skeleton, we find that the optimized molecules can realize both high triplet energies and balanced carrier transport properties with obvious TADF properties. The sky-blue PHOLEDs with

ultralow phosphor doping ratio employing **BPCN-Cz2Ph**, **BPCN-2Cz**, and **BPCN-3Cz** as host materials demonstrate really high performance with alleviated roll-offs and achieve impressive current efficiencies (CEs) of 46.5 cd A^{-1}, 50.0 cd A^{-1}, and 34.5 cd A^{-1}, power efficiencies (PEs) of 40.6 lm W^{-1}, 46.8 lm W^{-1}, and 34.8 lm W^{-1}, and external quantum efficiencies (EQEs) of 22.2%, 24%, and 15.8%, respectively. More encouragingly, even at an applied luminance of 1000 cd m^{-2}, the EQEs could maintain high levels of 21.0%, 21.5% and 12.8%, respectively, which represents the potential utility value of the new family of these molecules in blue PHOLEDs. Our molecular design strategy provides a practical way to construct promising wide-bandgap TADF host materials with an excellent combination of TADF property, high triplet energy, and balanced carrier-transporting ability for high-performance devices.

Keywords: thermally activated delayed fluorescence, bipolar host molecule, blue organic light-emitting diodes

1 Introduction

Blue emission takes a significantly important role in the three primary colors (RGB) based organic light-emitting diodes (OLEDs).[1-5] A great challenge still exists for researchers to achieve high-efficiency blue OLEDs owing to many strict requirements and corresponding difficulties.[3, 6-8] Nowadays, phosphorescent dyes have drawn tremendous attention worldwide due to their excellent exciton-harvesting ability in electroluminescence performance, realizing approximately 100% internal quantum efficiency (IQE).[9-11] Therefore, blue phosphorescent organic light-emitting diodes (PHOLEDs) outstand unparalleled merits in blue emission field of organic optoelectronic devices.[12-20] However, in spite of promising performance, the required high doping ratio of noble-metal based phosphorescent dyes in device fabrication is still

problematic considering the resource rarity.[21, 22] Fortunately, host materials with thermally activated delayed fluorescence (TADF) characteristics have become fashionable to relieve this stressed condition due to their effective reverse intersystem crossing (RISC) process and efficient resonance energy transfer to the dopants.[23-29] In general, phosphorescent dyes are normally dispersed in host molecular matrix to suppress the concentration quenching.[30, 31] An ideal host for phosphorescent dyes should fulfill the following demands[32, 33]: (1) a high triplet energy (E_T) level sufficient for impeding the reserve energy transfer; (2) high thermal stability; (3) reasonable highest occupied molecular orbital (HOMO) and lowest unoccupied molecular orbital (LUMO) to match frontier molecular orbitals of its adjacent charge transport molecules; (4) balanced hole-/electron- transporting properties to pursue efficient generation process of excitons. As we can see, first of all, a high triplet excited state for confining excitons on the phosphorescent molecules is essential to host materials.[34] It is a general way to increase the E_T by decreasing the π-conjugation length of molecules. However, the reduction in the conjugation length always takes a heavy toll on the charge transport properties.[35] Therefore, high E_T and high charge transport property are contradictory. Particularly, for blue emitters with a relatively high E_T, this strict requirement becomes a challenge for molecular design and limits the diversity of host molecules prepared for blue OLEDs.[36, 37]

Carbazole is a well-known electron donor with high E_T (3.0 eV) and many carbazole derivative wide-bandgap host materials have been developed.[38-45] The triplet energy level is very sensitive to the extension of the molecular π-conjugation. For instance, in contrast to the origin of carbazole, a conventional host material CBP has a sharp decrease in the E_T to be 2.5 eV, which is too low to afford the host for blue dyes. By reducing the π-conjugation of the carbazole moieties and the biphenyl units, two isomers *m*-CBP and *o*-CBP could again result in

higher E_Ts of 2.84 and 3.00 eV due to the limited conjugation length.[46] Therefore, tunable E_T energy could be realized by exactly controlling the π-conjugation length of carbazole moieties and the π-conjugation length need to be strictly limited for a wide-bandgap host molecule with high E_T. On the other hand, considering carrier transport property of a host molecule, a sufficient π-conjugation system of carbazole-units is another requirement that should be fulfilled in the molecular design. Otherwise, it may induce unbalanced hole-/electron- transporting property and thus a deficient process of exciton generation.

Herein, we report three wide-bandgap TADF host materials utilizing a benzene ring to combine carbazole derivative electron donors with high E_T and CN substituted benzene acceptor with electron withdrawing character to give new bipolar host materials of 4'-(3,6-diphenyl-9*H*-carbazol-9-yl)-[1,1'-biphenyl]-2-carbonitrile (**BPCN-Cz2Ph**), 4'-(9'-phenyl-9*H*,9'*H*-[3,3'-bicarbazol]-9-yl)-[1,1'-biphenyl]-2-carbonitrile (**BPCN-2Cz**), and 4'-(9,9''-diphenyl-9*H*,9'*H*,9''*H*-[3,3':6',3''-tercarbazol]-9'-yl)-[1,1'-biphenyl]-2-carbonitrile (**BPCN-3Cz**). By modulation of the carbazole units in the molecular skeleton frame, tunable bandgap and bipolarity, appropriate highest occupied molecular orbital (HOMO) energy level, small singlet-triplet splitting (ΔE_{ST}), high triplet energy, and balanced hole-/electron- transporting ability could be achieved. These three molecules designed on the same platform show impressively high performance when they are used as the host for sky-blue PHOLEDs with ultralow iridium(III) bis(4,6-(difluorophenyl)pyridinato-N,C2′)picolinate (FIrpic) doping ratio (5 wt%). The devices hosted by **BPCN-Cz2Ph**, **BPCN-2Cz** and **BPCN-3Cz** respectively achieved current efficiencies (CEs) of 46.5 cd A^{-1}, 50.0 cd A^{-1} and 34.5 cd A^{-1}, power efficiencies (PEs) of 40.6 lm W^{-1}, 46.8 lm W^{-1} and 34.8 lm W^{-1}, and external quantum efficiencies (EQEs) of 22.2%, 24% and 15.8%. More encouragingly, even at an applicable luminance of 1000 cd m^{-2}, the EQEs could maintain high

levels of 21.0%, 21.5% and 12.8%, respectively, which represents the potential utility value of this new family of host molecules in blue PHOLEDs. By optimizing the carbazole derivative donor segments in the molecular skeleton, we could obtain ideal TADF host materials featured with both high E_Ts and balanced charge transport properties. This structural optimization method provides a practical way to build promising host materials for blue PHOLEDs and evidently confirm that an excellent combination of TADF property, high triplet energy, and balanced carrier transport capacity allow bipolar host materials to deliver a high performance.

2 Results and discussion

2.1 Synthesis and characterization

The synthetic processes of **BPCN-Cz2Ph**, **BPCN-2Cz** and **BPCN-3Cz** are described in **Scheme 1**. The di/tri-carbazole precursors 9-phenyl-9*H*,9'*H*-3,3'-bicarbazole (**2**) and 9,9"-diphenyl-9*H*,9'*H*,9"*H*-3,3':6',3"-tercarbazole (**3**) were prepared according to the literature.[47-49] The final products can be obtained via Buchwald-Hartwig cross coupling reaction between related carbazole derivatives (**1**, **2**, **3**) and 4'-chloro-[1,1'-biphenyl]-2-carbonitrile. The complexes were fully identified by $^{1}H/^{13}C$ NMR, MALDI-TOF mass spectrometry and elemental analysis (**Fig. S8-S15**).

2.2 Theoretical calculations

To primarily get insight in the electronic structure of **BPCN-Cz2Ph**, **BPCN-2Cz** and **BPCN-3Cz**, density function theory (DFT) calculations were carried out to simulate the frontier orbitals of HOMO/LUMO distributions of these three molecules as shown in **Fig. 1**. We can see that the electron clouds of HOMOs were mainly spread on the donor moiety- 3,6-diphenyl-9*H*-carbazole (Cz2Ph), 9-phenyl-9*H*,9'*H*-3,3'-bicarbazole (2Cz) and 9,9"-diphenyl-9*H*,9'*H*,9"*H*-3,3':6',3"-tercarbazole (3Cz) as well as central benzene motif for **BPCN-Cz2Ph**, **BPCN-2Cz** and **BPCN-**

3Cz, respectively, while LUMOs of these three compounds were found to be mostly located on the the acceptor moiety- the group of biphenyl carbonitrile (BPCN). The highly separated distributions of HOMO and LUMO would lead to a small ΔE_{ST} and an effective hole/electron transport route in these bipolar host materials, benefitting the upconversion process of RISC and the formation of excitons, respcetively. To investigate the characteristics of the lowest excited states (S_1 and T_1) of **BPCN-Cz2Ph**, **BPCN-2Cz** and **BPCN-3Cz**, we further used natural transition orbitals (NTO) analysis to study their excited states. As shown in **Fig. S1**, **BPCN-Cz2Ph**, **BPCN-2Cz** and **BPCN-3Cz** show very similar hole and electron distribution behavior in their S_1 states, the holes are mainly located on the Cz2Ph, 2Cz and 3Cz units, and electrons are mainly distributed on BPCN group. This typical S_1 state distribution of these three compounds suggests the characteristics of a charge transfer (CT) state, revealing the reason of their feature-less broad PL spectra. As depicted in **Fig. S2**, the T_1 holes are mostly located on the BPCN group and partially extended to the donor moieties. In addition, the T_1 electrons of these three compounds exhibit nearly the same distributions. This observation results in the hybrid CT and locally excited (LE) state of T_1 for **BPCN-Cz2Ph**, **BPCN-2Cz** and **BPCN-3Cz**.

2.3 Photophysical properties

To study the photophysical behaviors of **BPCN-Cz2Ph**, **BPCN-2Cz** and **BPCN-3Cz**, UV-Vis absorption and photoluminescence (PL) measurement were carried out. Firstly, at room temperature (RT), the absorption and fluorescence emission characteristics of **BPCN-Cz2Ph**, **BPCN-2Cz** and **BPCN-3Cz** were evaluated in toluene solution, and then low-temperature (77K) phosphorescent spectra were investigated in toluene glass matrix (**Fig. 2a**). Their experimental data are summarized in **Table 1**. **BPCN-Cz2Ph**, **BPCN-2Cz** and **BPCN-3Cz** show similar absorption feature with a strong absorption band around 296 nm for **BPCN-Cz2Ph** and 305 nm

for both **BPCN-2Cz** and **BPCN-3Cz**, which are deemed to be the intrinsic π-π* transitions, besides, the relatively weak absorption band in the range of 325–350 nm could be attributed to the transition of intramolecular charge-transfer (ICT). The resemble characteristics of absorption spectra can be explained by their similar molecular backbone used in **BPCN-Cz2Ph**, **BPCN-2Cz** and **BPCN-3Cz**. According to the absorption edges, the optical bandgaps (E_gs) can be estimated to be 3.35 eV for **BPCN-Cz2Ph**, 3.36 eV for **BPCN-2Cz** and 3.30 eV for **BPCN-3Cz**. On account of the strong electron-donating property of carbazole, it is easily understood that **BPCN-3Cz** showed a bathochromic-shift in its absorption spectra compared with those of **BPCN-Cz2Ph** and **BPCN-2Cz**. Thus, **BPCN-3Cz** would have the smallest bandgap among the three compounds. In the PL spectra, the feature-less broad emission peaked at 404 nm, 423 nm and 429 nm, corresponding to the singlet energies (E_Ss) of 3.07 eV, 2.93 eV, and 2.89 eV, were observed for **BPCN-Cz2Ph**, **BPCN-2Cz** and **BPCN-3Cz**, respectively. In the phosphorescent spectra (Phos), from the first vibrational peaks, the E_Ts of **BPCN-Cz2Ph**, **BPCN-2Cz** and **BPCN-3Cz** could be respectively determined to be 2.76 eV, 2.71 eV, and 2.72 eV. Due to the high enough E_T values, all the three molecules are inferred appropriate host materials for blue PHOLEDs. In the interest of gaining more insight into the ICT characteristics of these three molecules, the solvent-polarity-dependent PL was tested as shown in **Fig. 2b**. For **BPCN-Cz2Ph**, **BPCN-2Cz** and **BPCN-3Cz**, with the increasing polarity of solvent from low-polarity toluene to high-polarity DMF, obvious red-shift in the PL spectra of all the three molecules were observed, indicating extensive ICT characteristics in their excited states. To confirm if **BPCN-Cz2Ph**, **BPCN-2Cz**, and **BPCN-3Cz** possess TADF character in such small ΔE_{ST}s (0.31 eV, 0.22 eV, and 0.17 eV), the transient PL decay characteristics of **BPCN-Cz2Ph**/**BPCN-2Cz**/**BPCN-3Cz** neat films were investigated (**Fig. 2c**). All the neat films exhibit dual decay

characteristics with a short lifetime (τ_P) of 6.4/12.1/9.0 ns and a relatively long lifetime (τ_D) of 0.46/0.34/0.34 μs, corresponding to the prompt and delayed components of a typical TADF material. We also investigated their prompt and delayed fluorescence spectra using time-resolved PL spectra test (**Fig. S3**). Besides, photoluminescence quantum efficiency (η_{PL}) of their neat films were measured (78% for **BPCN-Cz2Ph**, 68% for **BPCN-2Cz**, 73% for **BPCN-3Cz**). In addtion, to verify the triplet exciton confinement ability of these current TADF hosts, we also performed the transient PL decay measurement of their doped films co-deposited with a well-known sky-blue triplet emitter of Firpic (**Fig. 2d**). Although all the co-deposited films didn't exhibit a mono-exponential decay curve, but its second exponential decay component is far fewer than the first exponential decay part, which indicates the triplet energy transfer from FIrpic to these host materials was successfully suppressed. The detailed data are summarized in **Table S1.** Among these doped films, η_{PL} of 91% was achieved for **BPCN-2Cz** in contrast with **BPCN-2Cz** (85%) and **BPCN-3Cz**(52%), which could be due to the more efficient host-guest energy transfer and good exciton-confinement on guest molecules. In addition, typical emission spectra of FIrpic were obtained (**Fig. S4**), indicating the direct and full radiation from T_1 of FIrpic. Last, we compared the absorption spectrum of FIrpic and PL spectra of **BPCN-Cz2Ph**, **BPCN-2Cz**, and **BPCN-3Cz** neat films (**Fig. S5**).

2.4 Thermal properties

High thermal stability is prerequisite for organic molecules as the host material in OLED fabrication and operation. To study the thermal stability of **BPCN-Cz2Ph**, **BPCN-2Cz** and **BPCN-3Cz**, thermogravimetric analyses (TGA) and differential scanning calorimetry (DSC) were performed (**Fig. 3**). All these molecules exhibited high thermal properties with the decomposition temperature (T_d, corresponding to 5 wt% loss) over 400 □ and glass transition

temperature (T_g) over 100 □. Their good thermal stability could be due to the rigid molecular skeleton frame of these three molecules. Particularly, carefully comparing the molecular configuration of these three molecules, **BPCN-Cz2Ph**, **BPCN-2Cz** and **BPCN-3Cz** show a relative relationship with T_d (408 □, 458 □ and 478 □) and T_g (101 □, 127 □ and 172 □). The synchronously increasing T_d and T_g along with the number of carbazole-units was observed, which can be explained by the increasing rigid carbazole-units in molecular skeleton frame. The excellent thermal stability suggests that **BPCN-Cz2Ph**, **BPCN-2Cz** and **BPCN-3Cz** could produce morphologically stable thin films during the thermal evaporation.

2.5 Electrochemical properties

The electrochemical properties of **BPCN-Cz2Ph**, **BPCN-2Cz** and **BPCN-3Cz** were studied via the cyclic voltammetry (CV) technique using ferrocene as the internal reference in degassed DCM (**Fig. S6**). From threshold of the electrochemical oxidation potential vs Fc^+/Fc, HOMO energy levels of **BPCN-Cz2Ph**, **BPCN-2Cz** and **BPCN-3Cz** were determined to be -5.49 eV, -5.25 eV, and -5.21eV, respectively. In addition, based on the empirical equation and the optical energy gap, LUMO energy levels of **BPCN-Cz2Ph**, **BPCN-2Cz** and **BPCN-3Cz** could be respectively estimated to be -2.14 eV, -1.89 eV, and -1.91 eV. The HOMO values of **BPCN-Cz2Ph**, **BPCN-2Cz** and **BPCN-3Cz** show a tendency to increase on account of the increasing electron-donating capability of the moiety- Cz2Ph, 2Cz and 3Cz. Since all these products contained the same electron-withdrawing moiety, it easily explained the tendency of reducing bandgap for the three compounds. The HOMOs and LUMOs of these host materials need to suitably match with frontier molecular orbitals of the neighboring layers to prefer the electron-hole pair recombination in the emitting layer (EML).

2.6 Electroluminescence (EL) properties

To evaluate the potential of **BPCN-Cz2Ph**, **BPCN-2Cz** and **BPCN-3Cz** as real host character, sky-blue PHOLEDs were fabricated with 5 wt% of FIrpic as a dopant via co-evaporation with **BPCN-Cz2Ph**, **BPCN-2Cz**, or **BPCN-3Cz**. It should be noted that the optimized doping concentration of 5 wt% FIrpic in these three host materials is much lower than the conventional doping values in the range of 15-20 wt%, which might be benefitted from the TADF characteristics of host molecules. The device configuration is depicted as following: indium tin oxide (ITO)/dipyrazino[2,3-*f*:2',3'-*h*]quinoxaline-2,3,6,7,10,11-hexacarbonitrile (HAT-CN) (10 nm)/1,1-bis[4-[N,N-di(p-tolyl)-amino]phenyl]cyclohexane (TAPC) (40 nm)/tris(4-(9H-carbazol-9-yl)phenyl)amine (TCTA) (10 nm)/Host: FIrpic (5 wt%, 20 nm)/1,3,5-tri[(3-pyridyl)-phen-3-yl]benzene (TmPyPB) (55 nm)/8-hydroxyquinolinolato lithium (Liq) (2 nm)/Al (120 nm). **Fig. 4a** shows the energy level diagrams, and the chemical structures of the molecules applied in the OLEDs are given in **Fig. 4e**. Here, HAT-CN and Liq were respectively used as hole-injecting layer (HIL) and electron-injecting layer (EIL). TAPC acted as hole-transporting layer (HTL). A 10-nm-thick TCTA was inserted between HTL and EML as electron-blocking layer (EBL). TmPyPB took roles of both electron-transporting layer (ETL) and hole-blocking layer (HBL) in the meantime. **Fig. 4c** depicts the current density-voltage-luminescence (*J-V-L*) curves of the PHOLEDs employing these three host materials. And the devices employing **BPCN-Cz2Ph**, **BPCN-2Cz** and **BPCN-3Cz** show relative low turn-on voltages at 100 cd m^{-2} of 3.60 V, 3.36 V, and 3.17 V, respectively. The slight difference might be due to the different HOMO/LUMO levels and charge transport ability of the three host molecules. To fully verify the bipolar property of **BPCN-Cz2Ph**, **BPCN-2Cz** and **BPCN-3Cz**, we have further fabricated hole-only devices (HODs) and electron-only devices (EODs) (**Fig. 5**). Based on space-charge-limited current (SCLC) model, the hole/electron mobilities of BPCN-Cz2Ph, BPCN-2Cz, and BPCN-

3Cz are calculated to be $7.77\times10^{-6}/1.57\times10^{-7}$, $9.94\times10^{-6}/3.65\times10^{-7}$, and $1.48\times10^{-5}/3.23\times10^{-6}$ cm^2 v^{-1} s^{-1}, respectively. **Fig. 4b,4d** give CE-*J*-PE, EQE-*J* characteristics of **BPCN-Cz2Ph**, **BPCN-2Cz** and **BPCN-3Cz** based sky-blue PHOLEDs. The device performances are summarized in **Table 2**. At 100 cd m^{-2}, the **BPCN-2Cz** based OLEDs achieved 50.0 cd A^{-1}, 46.8 lm W^{-1} and 24.0% of CE, PE and EQE, respectively, which are higher than those of **BPCN-Cz2Ph** (46.5 cd A^{-1}, 40.6 lm W^{-1} and 22.2%) and **BPCN-3Cz** (34.5 cd A^{-1}, 34.8 lm W^{-1} and 15.8%) based devices. To our knowledge, the superior device efficiency based on **BPCN-2Cz** are among the best values of FIrpic-based sky-blue PHOLEDs.[16, 50-63] In fact, **BPCN-Cz2Ph**, **BPCN-2Cz** and **BPCN-3Cz** all show triplet energies high enough to be host materials for FIrpic (2.62 eV). An efficient host-guest energy transfer from **BPCN-Cz2Ph**, **BPCN-2Cz** and **BPCN-3Cz** to FIrpic and a splendid triplet exciton confinement on the FIrpic molecules should be achieved. Thus, the slight difference in device performance should be due to the difference in electron-hole balance injection/transport in the EML, which is depended on the bipolar property of the host material. A nice host molecule not only possesses a high E_T to confine the excitons on dopant but also has a balanced carrier transport character to favor the recombination process of excitons in EML. In addition, at a high driving voltage in PHOLEDs, efficiency roll-off is a typical phenomenon and always be related to the quenching effect of triplet-triplet annihilation (TTA) and the triplet-polaron annihilation (TPA). In FIrpic-based sky-blue PHOLEDs, this efficiency roll-off could be alleviated by utilizing our new family of TADF molecules as the host materials. With the TADF nature of these three host materials, the up-conversion of triplet excitons to singlets will reduce the concentration of triplets, thus resulting in reduced TTA and TPA at high driving current density and smaller efficiency roll-off. Impressively, even at 1000 cd m^{-2}, the performances of **BPCN-2Cz** and **BPCN-CZ2Ph** based devices could maintain high levels of

44.8 cd A^{-1}, 34.5 lm W^{-1}, 21.5% and 44.2 cd A^{-1}, 32.6 lm W^{-1}, 21.0%, respectively. While for **BPCN-3Cz**, due to the unbalanced carrier transport ability at high driving voltage, **BPCN-3Cz** based devices showed a slightly high EQE roll-off of 19.0% from 100 cd m^{-2} to 1000 cd m^{-2} in contrast to **BPCN-2Cz** (10.4%) and **BPCN-CZ2Ph** (5.4%). The results indicate the critical importance of a well-balanced charge transport property for a host material. The typical FIrpic emission were observed in the electroluminescence (EL) spectra of **BPCN-Cz2Ph**, **BPCN-2Cz** and **BPCN-3Cz** based devices as shown in the inset of **Fig. 4d**, which means a well triplet energy confinement on the FIrpic molecules could be achieved by using **BPCN-Cz2Ph**, **BPCN-2Cz** and **BPCN-3Cz** as the host materials. Moreover, due to the increasing long-range Förster energy transfer from TADF host to guest, low doping ratio of dopants is needed. To verify this superiority of **BPCN-Cz2Ph**, **BPCN-2Cz** and **BPCN-3Cz**, we have fabricated sky-blue devices with higher doping concentration of 10 wt% and 15 wt% (**Fig. S7**). As we expected, the maximum EQEs of the **BPCN-Cz2Ph**, **BPCN-2Cz**, and **BPCN-3Cz** based devices with 10 wt% and 15 wt% doping concentrations were 19.1%/22.6%/15.6% and 18.8%/22.0%/15.3%, respectively. These results indicate that high performance could be achieved even at a low doping concentration like 5 wt% when using **BPCN-Cz2Ph**, **BPCN-2Cz**, and **BPCN-3Cz** as host.

3 Conclusions

In summary, a unique molecular design of TADF host materials has been demonstrated by combining carbazole electron-donors and CN substituted benzene electron-acceptor with a benzene ring. Excellent performance and reduced efficiency roll-off could be achieved in FIrpic-based PHOLEDs. Considering an ideal TADF host material should simultaneously fulfil the two

requirements: (1) a sufficiently high E_T, (2) a well-balanced carrier transport ability, we modulated the carbazole units in the novel molecular skeleton frame to study the influence of the increase in the number of the donor moieties on the molecular physical property. Although the family of these molecules could realize high E_T as host materials for FIrpic, slight difference in device performance was observed, which might be due to the difference in carrier transport ability of host materials. Based on these present findings, we believe our method of molecular design provides a practical way to construct promising host molecules and reveal device performance enhancement for blue PHOLEDs.

4 Experimental section

4.1 Synthesis of 4'-chloro-[1,1'-biphenyl]-2-carbonitrile

2-iodobenzonitrile (5 g, 21.8 mmol), (4-chlorophenyl)boronic acid (4.08 g, 26.16 mmol), K_2CO_3 (12.03 g, 87.2 mmol), and $Pd(PPh_3)_4$ (254 mg, 0.22 mmol) were dissolved in a 200 mL mixture of 1,4-dioxane and water (10/1, v/v) under argon atmosphere. The mixture was stirred for 24 h at 90 □ and cooled down to room temperature. Afterwards, the resulting mixture was mixed with 200 mL water and then dichloromethane was used to extract the desired product, which would be collected and evaporated under reduced pressure. After evaporation, the organic phase was further purified via column chromatography using petroleum ether and dichloromethane (3/1, v/v) as the eluent solvents to give a white solid (4.57 g, 98%). ^{1}H NMR (400 MHz, $CDCl_3$) δ 7.77 (d, J = 7.6 Hz, 1H), 7.66 (t, J = 7.7 Hz, 1H), 7.48 (tt, J = 4.6 Hz, 6H).

4.2 Synthesis of 3,6-diphenyl-9*H*-carbazole (1)

3,6-dibromo-9*H*-carbazole (2 g, 6.15 mmol), phenylboronic acid (1.80 g, 14.76 mmol), K_2CO_3 (3.4 g, 24.6 mmol), and $Pd(PPh_3)_4$ (208 mg, 0.18 mmol) were dissolved in a 100 mL mixture of 1,4-dioxane and water (10/1, v/v) under argon atmosphere. The mixture was stirred for 24 h at 90

□ and cooled down to room temperature. Afterwards, the resulting mixture was mixed with 200 mL water and then dichloromethane was used to extract the desired product, which would be collected and evaporated under reduced pressure. After evaporation, the organic phase was further purified via column chromatography using petroleum ether and dichloromethane (2/1, v/v) as the eluent solvents to afford 3,6-diphenyl-9H-carbazole a white solid (1.69 g, 86%). ^{1}H NMR (400 MHz, $CDCl_3$) δ 8.35 (s, 2H), 8.09 (s, 1H), 7.73 (t, *J* = 6.8 Hz, 5H), 7.69 (s, 1H), 7.49 (t, *J* = 7.2 Hz, 6H), 7.36 (t, *J* = 7.3 Hz, 2H).

4.3 Synthesis of 4'-(3,6-diphenyl-9*H*-carbazol-9-yl)-[1,1'-biphenyl]-2-carbonitrile (BPCN-Cz2Ph)

A mixture of **1** (1 g, 3.13mmol), 4'-chloro-[1,1'-biphenyl]-2-carbonitrile (805 mg, 3.76 mmol), $Pd_2(dba)_3$ (147 mg, 0.16 mmol), *s*-Phos (193 mg, 0.47 mmol) and *t*-BuONa (1.2 g, 12.52 mmol) was put in 100 mL toluene. The mixture was stirred and heated for 24 h at 110 □ under argon and cooled down to the room temperature. Then, dichloromethane was used to extract the resulting product. The combined organic extracts were dried over Na_2SO_4 and evaporated under reduced pressure. After evaporation, the product was purified via column chromatography on silica gel while using petroleum ether and dichloromethane (1/1, v/v) as the eluent solvents to afford **BPCN-Cz2Ph** a white solid (1.24 g, 80%). ^{1}H NMR (600 MHz, DMSO) δ 8.77 (s, 2H), 8.04 (d, *J* = 7.8 Hz, 1H), 7.93 (d, *J* = 7.8 Hz, 2H), 7.90 – 7.85 (m, 3H), 7.83 (d, *J* = 8.1 Hz, 5H), 7.80 (d, *J* = 11.6 Hz, 2H), 7.66 (t, *J* = 7.6 Hz, 1H), 7.57 (d, *J* = 8.6 Hz, 2H), 7.51 (t, *J* = 7.3 Hz, 4H), 7.37 (t, *J* = 7.3 Hz, 2H). ^{13}C NMR (151 MHz, $CDCl_3$) δ 144.41, 141.79, 140.49, 138.15, 137.06, 133.97, 133.91, 133.04, 130.40, 130.10, 128.80, 127.94, 127.32, 126.93, 126.66, 125.78, 124.22, 118.90, 118.68, 111.22, 110.26. MALDI-TOF-MS: m/z: calcd for $C_{37}H_{24}N_2$: 496.61,

found: 496.64. Anal. calcd for $C_{37}H_{24}N_2$ (%): C 89.49, H 4.87, N 5.64; found: C 89.28, H 4.96, N 5.58.

4.4 Synthesis of 4'-(9'-phenyl-9*H*,9'*H*-[3,3'-bicarbazol]-9-yl)-[1,1'-biphenyl]-2-carbonitrile (BPCN-2Cz)

The work-up procedures of **BPCN-2Cz** were similar to those used for **BPCN-Cz2Ph** to obtain a white solid (1.22 g, 85%). ^{1}H NMR (600 MHz, DMSO) δ 8.71 (d, *J* = 7.4 Hz, 2H), 8.41 (dd, *J* = 7.7 Hz, 2H), 8.04 (d, *J* = 7.8 Hz, 1H), 7.95 – 7.84 (m, 7H), 7.79 (d, *J* = 7.7 Hz, 1H), 7.71 (t, *J* = 7.6 Hz, 2H), 7.66 (dd, *J* = 8.0 Hz, 3H), 7.60 – 7.54 (m, 2H), 7.50 (q, *J* = 8.3 Hz, 3H), 7.46 (d, *J* = 7.5 Hz, 1H), 7.42 (d, *J* = 8.2 Hz, 1H), 7.35 (dt, *J* = 7.2 Hz, 2H). ^{13}C NMR (151 MHz, $CDCl_3$) δ 144.48, 141.33, 141.05, 140.03, 139.71, 138.33, 137.74, 136.92, 134.65, 134.23, 133.97, 133.03, 130.35, 130.11, 129.90, 127.89, 127.43, 127.05, 127.02, 126.20, 126.04, 125.94, 125.82, 124.19, 123.96, 123.77, 123.54, 120.47, 120.43, 120.30, 119.98, 118.92, 118.89, 118.70, 111.22, 110.11, 110.03, 109.98, 109.88. MALDI-TOF-MS: m/z: calcd for $C_{43}H_{27}N_3$: 585.71, found: 585.23. Anal. calcd for $C_{43}H_{27}N_3$ (%): C 88.18, H 4.65, N 7.17; found: C 87.98, H 4.78, N 7.13.

4.5 Synthesis of 4'-(9,9''-diphenyl-9*H*,9'*H*,9''*H*-[3,3':6',3''-tercarbazol]-9'-yl)-[1,1'-biphenyl]-2-carbonitrile (BPCN-3Cz)

The work-up procedures of **BPCN-3Cz** were similar to those used for **BPCN-Cz2Ph** to obtain a white solid (1.02 g, 80%). ^{1}H NMR (600 MHz, $CDCl_3$) δ 8.58 (s, 2H), 8.51 (s, 2H), 8.27 (d, *J* = 7.6 Hz, 2H), 7.87 (t, *J* = 6.9 Hz, 3H), 7.84 (t, *J* = 7.9 Hz, 6H), 7.75 (t, *J* = 7.5 Hz, 1H), 7.66 (d, *J* = 21.0 Hz, 11H), 7.54 (d, *J* = 8.0 Hz, 3H), 7.50 (s, 2H), 7.45 (q, *J* = 8.2 Hz, 4H), 7.33 (t, *J* = 7.0 Hz, 2H). ^{13}C NMR (151 MHz, $CDCl_3$) δ 144.69, 141.61, 140.44, 140.32, 138.70, 138.04, 137.12, 134.97, 134.44, 134.02, 132.98, 130.47, 130.20, 129.94, 127.94, 127.51, 127.23, 127.11, 126.16, 126.10, 125.93, 124.63, 124.18, 123.78, 120.50, 120.08, 119.11, 118.98, 118.61, 111.58, 110.32,

110.11, 109.96. MALDI-TOF-MS: m/z: calcd for $C_{61}H_{38}N_4$: 827.00, found: 826.31. Anal. calcd for $C_{61}H_{38}N_4$ (%): C 88.59, H 4.63, N 6.77; found: C 88.06, H 4.77 N 6.52.

Notes

The authors declare no competing financial interest.

Acknowledgements

The authors are funded by the National Natural Science Foundation of China (51821002, 61575136, and 21871199) and the National Key R&D Program of China (2016YFB0400700). "111" Project of The State Administration of Foreign Experts Affairs of China, Priority Academic Program Development of Jiangsu Higher Education Institutions (PAPD), and Collaborative Innovation Centre of Suzhou Nano Science and Technology (Nano-CIC) also provide the financial support to this work.

References

[1] J. Lee, H.F. Chen, T. Batagoda, C. Coburn, P.I. Djurovich, M.E. Thompson, S.R. Forrest, Deep blue phosphorescent organic light-emitting diodes with very high brightness and efficiency, Nat. Mater., 15 (2016) 92-98.

[2] Y. Zhang, J. Lee, S.R. Forrest, Tenfold increase in the lifetime of blue phosphorescent organic light-emitting diodes, Nat. Commun., 5 (2014) 5008.

[3] J. Lee, C. Jeong, T. Batagoda, C. Coburn, M.E. Thompson, S.R. Forrest, Hot excited state management for long-lived blue phosphorescent organic light-emitting diodes, Nat. Commun., 8 (2017) 15566.

[4] C.Y. Chan, M. Tanaka, H. Nakanotani, C. Adachi, Efficient and stable blue delayed fluorescence organic light-emitting diodes with CIEy below 0.4, Nat. Commun., 9 (2018) 5036.

[5] S. Lee, S.O. Kim, H. Shin, H.J. Yun, K. Yang, S.K. Kwon, J.J. Kim, Y.H. Kim, Deep-blue phosphorescence from perfluoro carbonyl-substituted iridium complexes, J. Am. Chem. Soc., 135 (2013) 14321-14328.

[6] P. Heimel, A. Mondal, F. May, W. Kowalsky, C. Lennartz, D. Andrienko, R. Lovrincic, Unicolored phosphor-sensitized fluorescence for efficient and stable blue OLEDs, Nat. Commun., 9 (2018) 4990.

[7] L.S. Cui, Y.M. Xie, Y.K. Wang, C. Zhong, Y.L. Deng, X.Y. Liu, Z.Q. Jiang, L.S. Liao, Pure hydrocarbon hosts for approximately 100% exciton harvesting in both phosphorescent and fluorescent light-emitting devices, Adv. Mater., 27 (2015) 4213-4217.

[8] Q. Wang, Y.X. Zhang, Y. Yuan, Y. Hu, Q.S. Tian, Z.Q. Jiang, L.S. Liao, Alleviating efficiency roll-off of hybrid single-emitting layer WOLED utilizing bipolar TADF material as host and emitter, ACS Appl. Mater. Interfaces, 11 (2019) 2197-2204.

[9] Y.-X. Zhang, B. Wang, Y. Yuan, Y. Hu, Z.-Q. Jiang, L.-S. Liao, Solution-processed thermally activated delayed fluorescence exciplex hosts for highly efficient blue organic light-emitting diodes, Adv. Opt. Mater., (2017) 1700012.

[10] W. Song, J.Y. Lee, Degradation mechanism and lifetime improvement strategy for blue phosphorescent organic light-emitting diodes, Adv. Opt. Mater., (2017) 1600901.

[11] A. B. Padmaperuma, L. S. Sapochak, P. E. Burrows, New charge transporting host material for short wavelength organic electrophosphorescence: 2,7-bis(diphenylphosphine oxide)-9,9-dimethylfluorene, *Chem. Mater.* 18 (2006), 2389-2396.

[12] S.O. Jeon, S.E. Jang, H.S. Son, J.Y. Lee, External quantum efficiency above 20% in deep blue phosphorescent organic light-emitting diodes, Adv. Mater., 23 (2011) 1436-1441.

[13] X. Li, J. Zhang, Z. Zhao, L. Wang, H. Yang, Q. Chang, N. Jiang, Z. Liu, Z. Bian, W. Liu, Z. Lu, C. Huang, Deep blue phosphorescent organic light-emitting diodes with CIEy value of 0.11 and external quantum efficiency up to 22.5%, Adv. Mater., 30 (2018) 1705005.

[14] A.K. Pal, S. Krotkus, M. Fontani, C.F.R. Mackenzie, D.B. Cordes, A.M.Z. Slawin, I.D.W. Samuel, E. Zysman-Colman, High-efficiency deep-blue-emitting organic light-emitting diodes based on Iridium(III) carbene complexes, Adv. Mater., 30 (2018) 1804231.

[15] H. Sasabe, J. Takamatsu, T. Motoyama, S. Watanabe, G. Wagenblast, N. Langer, O. Molt, E. Fuchs, C. Lennartz, J. Kido, High-efficiency blue and white organic light-emitting devices incorporating a blue iridium carbene complex, Adv. Mater., 22 (2010) 5003-5007.

[16] Y. Seino, H. Sasabe, Y.J. Pu, J. Kido, High-performance blue phosphorescent OLEDs using energy transfer from exciplex, Adv. Mater., 26 (2014) 1612-1616.

[17] H. Shin, Y.H. Ha, H.G. Kim, R. Kim, S.K. Kwon, Y.H. Kim, J.J. Kim, Controlling horizontal dipole orientation and emission spectrum of Ir complexes by chemical design of ancillary ligands for efficient deep-blue organic light-emitting diodes, Adv. Mater., 31 (2019) 1808102.

[18] H. Shin, J.H. Lee, C.K. Moon, J.S. Huh, B. Sim, J.J. Kim, Sky-blue phosphorescent OLEDs with 34.1% external quantum efficiency using a low refractive index electron transporting layer, Adv. Mater., 28 (2016) 4920-4925.

[19] K. Udagawa, H. Sasabe, C. Cai, J. Kido, Low-driving-voltage blue phosphorescent organic light-emitting devices with external quantum efficiency of 30%, Adv. Mater., 26 (2014) 5062-5066.

[20] L. Ding, S.-C. Dong, Z.-Q. Jiang, H. Chen, L.-S. Liao, Orthogonal molecular structure for better host material in blue phosphorescence and larger OLED white lighting panel, Adv. Funct. Mater., 25 (2015) 645-650.

[21] Y.-K. Wang, Q. Sun, S.-F. Wu, Y. Yuan, Q. Li, Z.-Q. Jiang, M.-K. Fung, L.-S. Liao, Thermally activated delayed fluorescence material as host with novel spiro-based skeleton for high power efficiency and low roll-off blue and white phosphorescent devices, Adv. Funct. Mater., 26 (2016) 7929-7936.

[22] Y.-K. Wang, S.-H. Li, S.-F. Wu, C.-C. Huang, S. Kumar, Z.-Q. Jiang, M.-K. Fung, L.-S. Liao, Tilted spiro-type thermally activated delayed fluorescence host for ≈100% exciton harvesting in red phosphorescent electronics with ultralow doping ratio, Adv. Funct. Mater., 28 (2018) 1706228.

[23] Z. Wu, L. Yu, X. Zhou, Q. Guo, J. Luo, X. Qiao, D. Yang, J. Chen, C. Yang, D. Ma, Management of singlet and triplet excitons: a universal approach to high-efficiency all fluorescent WOLEDs with reduced efficiency roll-off using a conventional fluorescent emitter, Adv. Opt. Mater., 4 (2016) 1067-1074.

[24] D. Zhang, M. Cai, Y. Zhang, D. Zhang, L. Duan, Highly efficient simplified single-emitting-layer hybrid WOLEDs with low roll-off and good color stability through enhanced Forster energy transfer, ACS Appl. Mater. Interfaces, 7 (2015) 28693-28700.

[25] J. Liang, C. Li, X. Zhuang, K. Ye, Y. Liu, Y. Wang, Novel blue bipolar thermally activated delayed fluorescence material as host emitter for high-efficiency hybrid warm-white OLEDs with stable high color-rendering index, Adv. Funct. Mater., 28 (2018) 1707002.

[26] Z. He, C. Wang, J. Zhao, X. Du, H. Yang, P. Zhong, C. Zheng, H. Lin, S. Tao, X. Zhang, Blue and white solution-processed TADF-OLEDs with over 20% EQE, low driving voltages and

moderate efficiency decrease based on interfacial exciplex hosts, J. Mater. Chem. C, 7 (2019) 11806-11812.

[27] J. Zhao, C. Zheng, Y. Zhou, C. Li, J. Ye, X. Du, W. Li, Z. He, M. Zhang, H. Lin, S. Tao, X. Zhang, Novel small-molecule electron donor for solution-processed ternary exciplex with 24% external quantum efficiency in organic light-emitting diode, Mater. Horiz., 6 (2019) 1425-1432.

[28] D. Zhang, L. Duan, D. Zhang, Y. Qiu, Towards ideal electrophosphorescent devices with low dopant concentrations: the key role of triplet up-conversion, J. Mater. Chem. C, 2 (2014) 8983-8989.

[29] H. Wang, L. Meng, X. Shen, X. Wei, X. Zheng, X. Lv, Y. Yi, Y. Wang, P. Wang, Highly efficient orange and red phosphorescent organic light-emitting diodes with low roll-off of efficiency using a novel thermally activated delayed fluorescence material as host, Adv. Mater., 27 (2015) 4041-4047.

[30] X.Y. Liu, Y.L. Zhang, X. Fei, L.S. Liao, J. Fan, 9,9'-Bicarbazole: new molecular skeleton for organic light-emitting diodes, Chem.-Eur. J., 25 (2019) 4501-4508.

[31] Q. Ran, Y.-L. Zhang, X. Hua, M.-K. Fung, L.-S. Liao, J. Fan, Modulation of p-type units in tripodal bipolar hosts towards highly efficient red phosphorescent OLEDs, Dyes Pigm., 162 (2019) 632-639.

[32] X.-D. Zhu, Y.-L. Zhang, Y. Yuan, Q. Zheng, Y.-J. Yu, Y. Li, Z.-Q. Jiang, L.-S. Liao, Incorporating a tercarbazole donor in a spiro-type host material for efficient RGB phosphorescent organic light-emitting diodes, J. Mater. Chem. C, 7 (2019) 6714-6720.

[33] Y.-L. Zhang, Q. Ran, Q. Wang, J. Fan, L.-S. Liao, High-efficiency exciplex-based white organic light-emitting diodes with a new tripodal material as a co-host, J. Mater. Chem. C, 7 (2019) 7267-7272.

[34] S.-J. Su, C. Cai, J. Kido, Three-carbazole-armed host materials with various cores for RGB phosphorescent organic light-emitting diodes, J. Mater. Chem., 22 (2012) 3447-3456.

[35] M.H. Tsai, H.W. Lin, H.C. Su, T.H. Ke, C.c. Wu, F.C. Fang, Y.L. Liao, K.T. Wong, C.I. Wu, Highly efficient organic blue electrophosphorescent devices based on 3,6-bis(triphenylsilyl)carbazole as the host material, Adv. Mater., 18 (2006) 1216-1220.

[36] X. Lv, W. Zhang, D. Ding, C. Han, Z. Huang, S. Xiang, Q. Zhang, H. Xu, L. Wang, Integrating the emitter and host characteristics of donor-acceptor systems through edge-spiro effect toward 100% exciton harvesting in blue and white fluorescence diodes, Adv. Opt. Mater., 6 (2018) 1800165.

[37] Q. Liang, C. Han, C. Duan, H. Xu, Blue thermally activated delayed fluorescence-emitting phosphine oxide hosts for ultrasimple and highly efficient white organic light-emitting diodes, Adv. Opt. Mater., 6 (2018) 1800020.

[38] S.-J. Su, H. Sasabe, T. Takeda, J. Kido, Pyridine-containing bipolar host materials for highly efficient blue phosphorescent OLEDs, Chem. Mater. 20 (2008) 1691-1693.

[39] J.K. Bin, N.S. Cho, J.I. Hong, New host material for high-performance blue phosphorescent organic electroluminescent devices, Adv. Mater., 24 (2012) 2911-2915.

[40] H.H. Chou, C.H. Cheng, A highly efficient universal bipolar host for blue, green, and red phosphorescent OLEDs, Adv. Mater., 22 (2010) 2468-2471.

[41] C.W. Lee, J.Y. Lee, Above 30% external quantum efficiency in blue phosphorescent organic light-emitting diodes using pyrido[2,3-b]indole derivatives as host materials, Adv. Mater., 25 (2013) 5450-5454.

[42] A. Maheshwaran, V.G. Sree, H.-Y. Park, H. Kim, S.H. Han, J.Y. Lee, S.-H. Jin, High efficiency deep-blue phosphorescent organic light-emitting diodes with CIE x, y (≤ 0.15) and low efficiency roll-off by employing a high triplet energy bipolar host material, Adv. Funct. Mater., 28 (2018) 1802945.

[43] S.J. Su, E. Gonmori, H. Sasabe, J. Kido, Highly efficient organic blue-and white-light-emitting devices having a carrier- and exciton-confining structure for reduced efficiency roll-off, Adv. Mater., 20 (2008) 4189-4194.

[44] S.O. Jeon, K.S. Yook, C.W. Joo, J.Y. Lee, Phenylcarbazole-based phosphine oxide host materials for high efficiency in deep blue phosphorescent organic light-emitting diodes, Adv. Funct. Mater., 19 (2009) 3644-3649.

[45] K.S. Yook, J.Y. Lee, Organic materials for deep blue phosphorescent organic light-emitting diodes, Adv. Mater., 24 (2012) 3169-3190.

[46] S. Gong, X. He, Y. Chen, Z. Jiang, C. Zhong, D. Ma, J. Qin, C. Yang, Simple CBP isomers with high triplet energies for highly efficient blue electrophosphorescence, J. Mater. Chem., 22 (2012) 2894-2899.

[47] X. Lv, B. Wang, J. Tan, Z. Huang, Q. Zhang, S. Xiang, W. Liu, S. Zhuang, L. Wang, Constructing diazacarbazole-bicarbazole bipolar hybrids by optimizing the linker group for high efficiency, low roll off electrophosphorescent devices, Dyes Pigm., 136 (2017) 54-62.

[48] K. Shizu, H. Noda, H. Tanaka, M. Taneda, M. Uejima, T. Sato, K. Tanaka, H. Kaji, C. Adachi, Highly efficient blue electroluminescence using delayed-fluorescence emitters with

large overlap density between luminescent and ground states, J. Phys. Chem. C, 119 (2015) 26283-26289.

[49] W. Zhang, Y.-X. Zhang, X.-Q. Zhang, X.-Y. Liu, J. Fan, L.-S. Liao, Blue thermally activated delayed fluorescence materials based on bi/tri-carbazole derivatives, Org. Electron., 58 (2018) 238-244.

[50] X. Yang, G. Zhou, W.Y. Wong, Functionalization of phosphorescent emitters and their host materials by main-group elements for phosphorescent organic light-emitting devices, Chem. Soc. Rev., 44 (2015) 8484-8575.

[51] L.J. Sicard, H.C. Li, Q. Wang, X.Y. Liu, O. Jeannin, J. Rault-Berthelot, L.S. Liao, Z.Q. Jiang, C. Poriel, C1-linked spirobifluorene dimers: pure hydrocarbon hosts for high-performance blue phosphorescent OLEDs, Angew. Chem. Int. Ed. Engl., 58 (2019) 3848-3853.

[52] Q.S. Tian, L. Zhang, Y. Hu, S. Yuan, Q. Wang, L.S. Liao, High-performance white organic light-emitting diodes with simplified structure incorporating novel exciplex-forming host, ACS Appl. Mater. Interfaces, 10 (2018) 39116-39123.

[53] Y. Zhao, C. Wu, P. Qiu, X. Li, Q. Wang, J. Chen, D. Ma, New benzimidazole-based bipolar hosts: highly efficient phosphorescent and thermally activated delayed fluorescent organic light-emitting diodes employing the same device structure, ACS Appl. Mater. Interfaces, 8 (2016) 2635-2643.

[54] M.M. Xue, C.C. Huang, Y. Yuan, L.S. Cui, Y.X. Li, B. Wang, Z.Q. Jiang, M.K. Fung, L.S. Liao, De novo design of boron-based host materials for highly efficient blue and white phosphorescent OLEDs with low efficiency roll-off, ACS Appl. Mater. Interfaces, 8 (2016) 20230-20236.

[55] F. Wang, D. Liu, J. Li, M. Ma, Modulation of n-type units in bipolar host materials toward high-performance phosphorescent OLEDs, ACS Appl. Mater. Interfaces, 9 (2017) 37888-37897.

[56] B. Pan, B. Wang, Y. Wang, P. Xu, L. Wang, J. Chen, D. Ma, A simple carbazole-N-benzimidazole bipolar host material for highly efficient blue and single layer white phosphorescent organic light-emitting diodes, J. Mater. Chem. C, 2 (2014) 2466-2469.

[57] X.-Y. Liu, Q.-S. Tian, D. Zhao, J. Fan, L.-S. Liao, Novel o-D-π-A arylamine/arylphosphine oxide hybrid hosts for efficient phosphorescent organic light-emitting diodes, Org. Electron., 56 (2018) 186-191.

[58] X.-Y. Liu, X. Tang, Y. Zhao, D. Zhao, J. Fan, L.-S. Liao, Spirobi[dibenzo[b,e][1,4]azasiline]: a novel platform for host materials in highly efficient organic light-emitting diodes, J. Mater. Chem. C, 6 (2018) 1023-1030.

[59] H. Liu, G. Cheng, D. Hu, F. Shen, Y. Lv, G. Sun, B. Yang, P. Lu, Y. Ma, A highly efficient, blue-phosphorescent device based on a wide-bandgap host/FIrpic: rational design of the carbazole and phosphine oxide moieties on tetraphenylsilane, Adv. Funct. Mater., 22 (2012) 2830-2836.

[60] C.-C. Lin, M.-J. Huang, M.-J. Chiu, M.-P. Huang, C.-C. Chang, C.-Y. Liao, K.-M. Chiang, Y.-J. Shiau, T.-Y. Chou, L.-K. Chu, H.-W. Lin, C.-H. Cheng, Molecular design of highly efficient thermally activated delayed fluorescence hosts for blue phosphorescent and fluorescent organic light-emitting diodes, Chem. Mater., 29 (2017) 1527-1537.

[61] W. Li, J. Li, F. Wang, Z. Gao, S. Zhang, Universal host materials for high-efficiency phosphorescent and delayed-fluorescence OLEDs, ACS Appl. Mater. Interfaces, 7 (2015) 26206-26216.

[62] C.L. Bian, Q. Wang, Q. Ran, X.Y. Liu, J. Fan, L.S. Liao, New carbazole-based bipolar hosts for efficient blue phosphorescent organic light-emitting diodes, Org. Electron., 52 (2018) 138-145.

[63] C. Bian, Q. Wang, X.-Y. Liu, J. Fan, L.-S. Liao, Orthogonally substituted aryl derivatives as bipolar hosts for blue phosphorescent organic light-emitting diodes, Org. Electron., 46 (2017) 105-114.

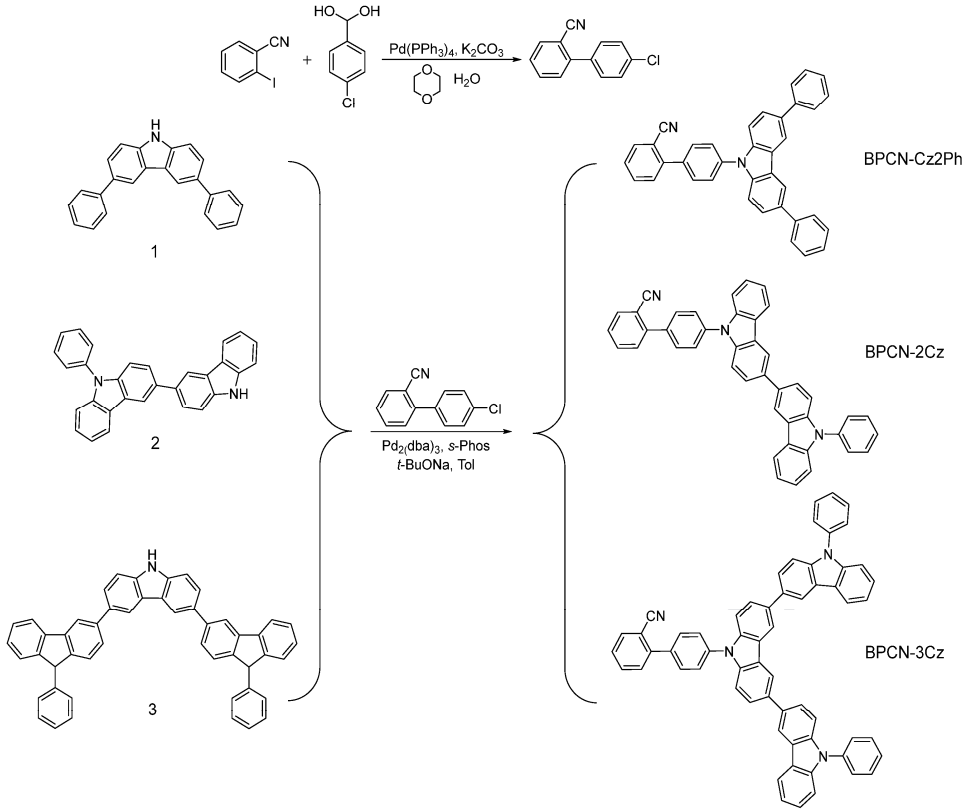

Scheme 1. The synthetic route of **BPCN-Cz2Ph**, **BPCN-2Cz** and **BPCN-3Cz**.

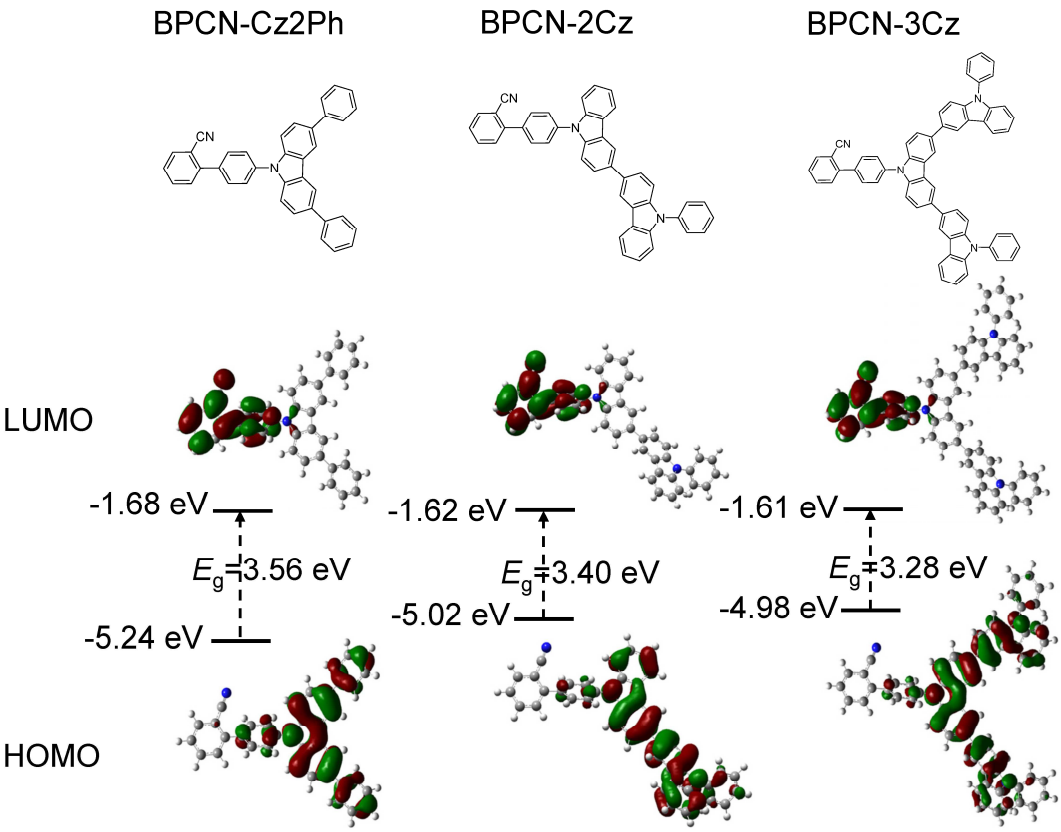

Fig. 1. Theoretically calculated spatial distributions and energy levels of the HOMO and LUMO of **BPCN-Cz2Ph**, **BPCN-2Cz** and **BPCN-3Cz** as well as their values of E_g.

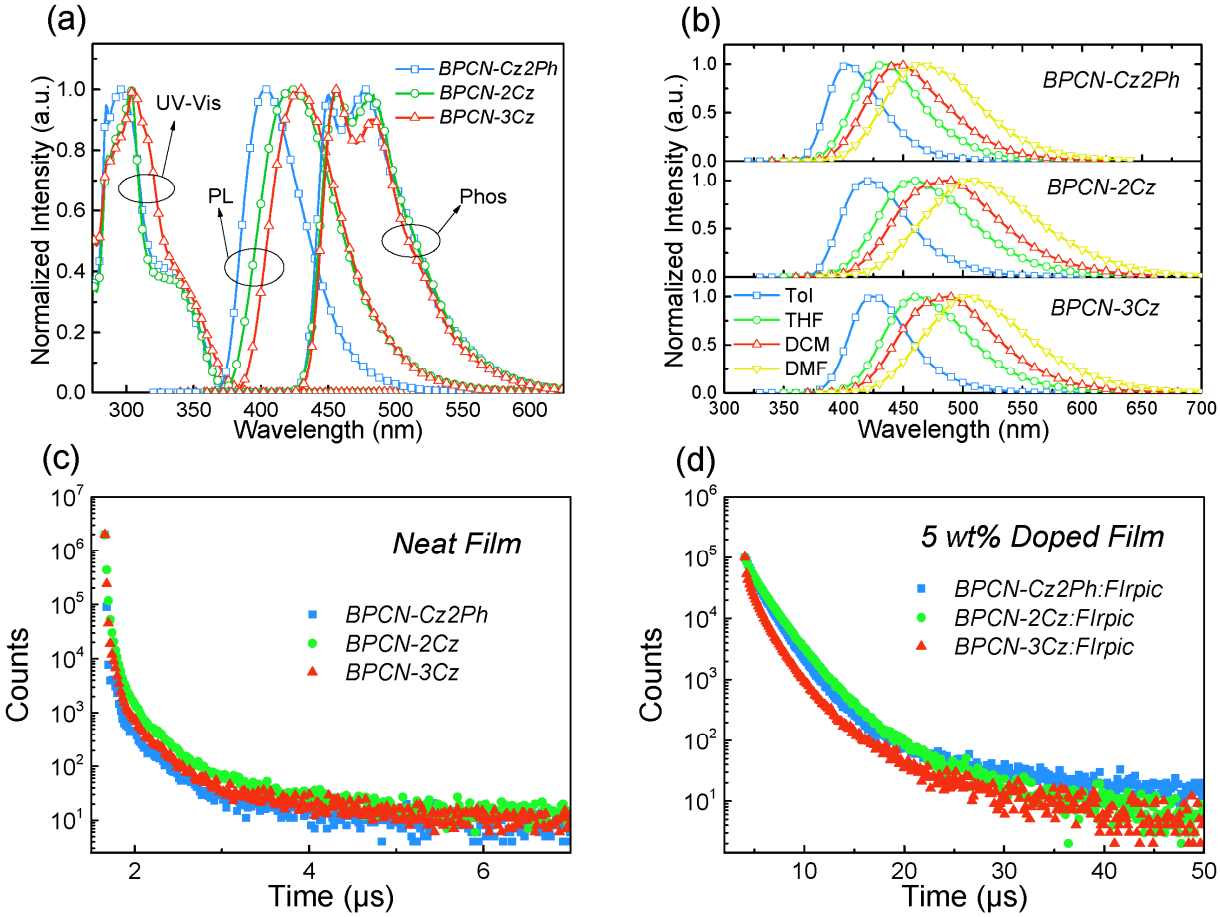

Fig. 2. (a) The absorption spectra (UV-Vis), photoluminescence spectra (PL) in toluene solution at room temperature (RT) and phosphorescent spectra (Phos) in toluene glass matrix at 77 K of **BPCN-Cz2Ph**, **BPCN-2Cz** and **BPCN-3Cz**. (b) The PL spectra of **BPCN-Cz2Ph**, **BPCN-2Cz**, and **BPCN-3Cz** in different solvents. (c, d) The transient PL decay curves of **BPCN-Cz2Ph**, **BPCN-2Cz**, and **BPCN-3Cz** neat films and 5 wt%-FIrpic-doped films.

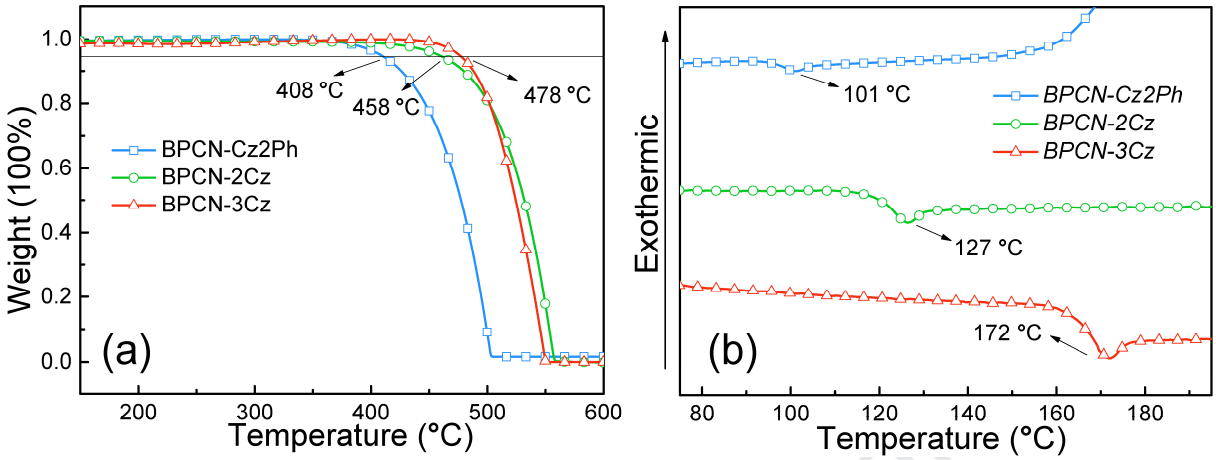

Fig. 3. The TGA and DSC curves of **BPCN-Cz2Ph**, **BPCN-2Cz** and **BPCN-3Cz** at 10 °C min^{-1} under nitrogen.

Table 1. Physical properties of **BPCN-Cz2Ph**, **BPCN-2Cz** and **BPCN-3Cz**.

Compounds	T_g[a] [□]	T_d[b] [□]	S_1 [eV]	T_1 [eV]	ΔE_{ST} [eV]	HOMO[c] [eV]	LUMO[d] [eV]	E_g[e] [eV]
BPCN-Cz2Ph	101	408	3.07	2.76	0.31	-5.49	-2.14	3.35
BPCN-2Cz	127	458	2.93	2.71	0.22	-5.25	-1.89	3.36
BPCN-3Cz	172	478	2.89	2.72	0.17	-5.21	-1.91	3.30

[a]T_g = temperature for glass-transition; [b]T_d = temperature for 5 wt.% loss; [c]HOMO measured by cyclic voltammetry (CV); [d]LUMO deduced from E_g and HOMO; [e]E_g = energy gap calculated by the onset absorption band.

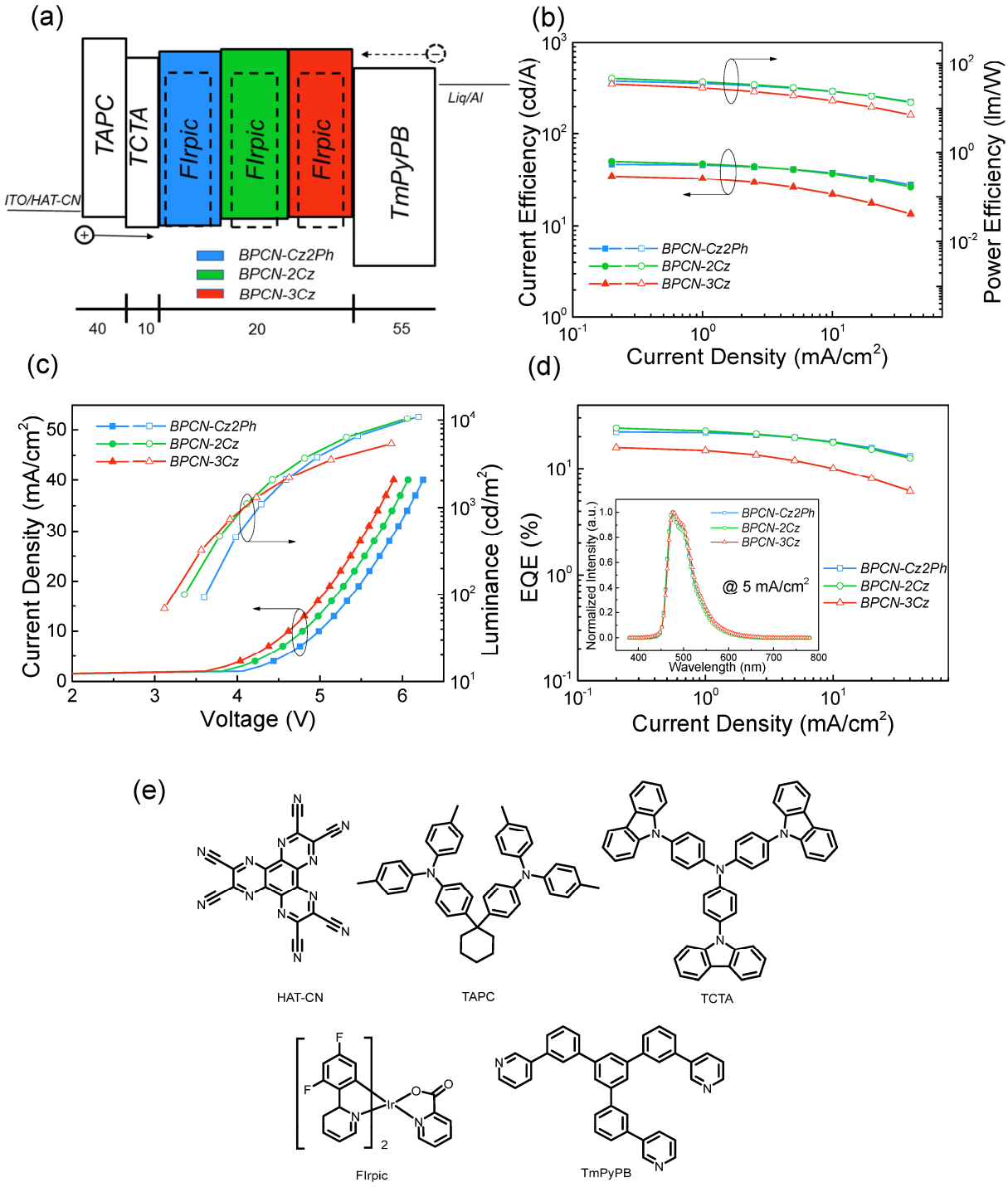

Fig. 4. EL characteristics of **BPCN-Cz2Ph**-, **BPCN-2Cz**-, and **BPCN-3Cz**-based OLEDs. (a) Schematic diagram of the device structure and energy level. (b) CE-*J*-PE curves. (c) *J*-*V*-*L*

curves. (d) EQE-*J* curves (inset: EL spectra at 5 mA cm^{-2}). (e) chemical structures of the materials employed in the devices.

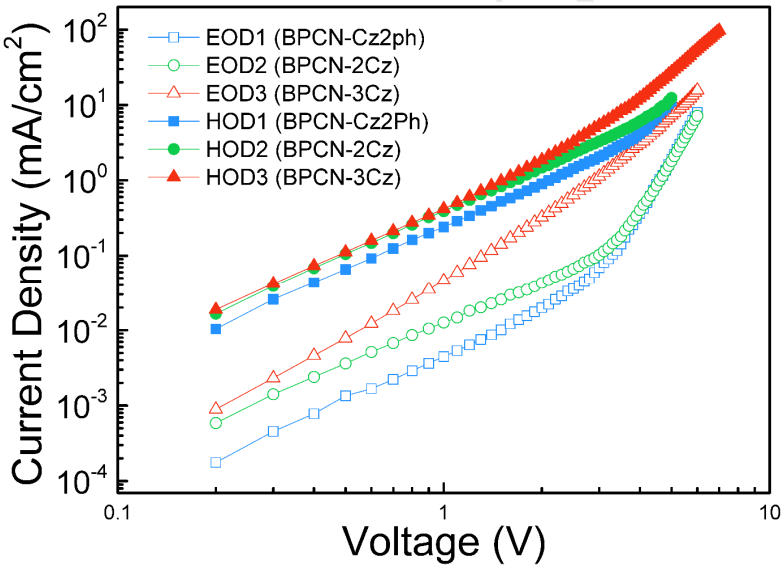

Fig. 5. *J-V* curves of hole-only device (ITO/HAT-CN (10 nm)/Host (100 nm)/HAT-CN (10 nm)/Al (120 nm)) and electron-only device (ITO/Liq (2 nm)/Host (100 nm)/Liq (2 nm)/Al (120 nm)).

Table 2. Device performance of blue PHOLEDs based on **BPCN-Cz2Ph**, **BPCN-2Cz** and **BPCN-3Cz**.

Device	V_{on} [a] [V]	CE [b] [cd A^{-1}]	PE [b] [lm W^{-1}]	EQE [b] [%]	CIE [c] (x, y)
BPCN-Cz2Ph	3.60	46.5, 46.3, 45.8, 44.2, 35.7, 28.7	40.6, 39.3, 35.9, 32.6, 21.7, 15.1	22.2, 22.0, 21.8, 21.0, 17.0, 13.7	(0.15, 0.36)
BPCN-2Cz	3.36	50.0, 49.3, 47.0, 44.8, 34.3, 26.9	46.8, 44.7, 38.9, 34.5, 21.5, 14.2	24.0, 23.6, 22.6, 21.5, 16.5, 12.9	(0.15, 0.35)
BPCN-3Cz	3.17	34.5, 33.5, 31.2, 27.9, 14.3, -	34.8, 31.6, 26.5, 21.8, 7.9, -	15.8, 15.3, 14.3, 12.8, 6.5,-	(0.16, 0.38)

[a] V_{on} at 100 cd m^{-2}; [b] CE, PE and EQE at 100, 200, 500, 1000, 5000 and 10000 cd m^{-2}, respectively; [c] CIE coordinates recorded at 5 mA cm^{-2}.

Supporting Information

High-Performance Sky-Blue Phosphorescent Organic Light-Emitting Diodes Employing Wide-Bandgap Bipolar Host Materials with Thermally Activated Delayed Fluorescence Characteristics

Yuan-Lan Zhang,[1,†] Quan Ran,[1,†] Qiang Wang,[1] Qi-Sheng Tian,[1] Fan-Cheng Kong,[1] Jian Fan,[1,2,] and Liang-Sheng Liao[1,2,]**

[1]Institute of Functional Nano & Soft Materials (FUNSOM), Jiangsu Key Laboratory for Carbon-Based Functional Materials & Devices, Soochow University, Suzhou, Jiangsu 215123, P. R. China.

[2]Institute of Organic Optoelectronics, Jiangsu Industrial Technology Research Institute (JITRI), Wujiang, Suzhou, Jiangsu 215211, P. R. China.

E-mail: lsliao@suda.edu.cn; jianfan@suda.edu.cn

†These two authors contributed equally to this work.

Materials and methods

All chemicals and reagents were used as received from commercial sources without further purification. ^{1}H NMR and ^{13}C NMR spectra were obtained on a Bruker 400 spectrometer and Agilent DD2-600 MHz NMR spectrometer. Matrix-Assisted Laser Desorption/ Ionization Time of Flight Mass Spectrometry (MALDI-TOF-MS) was measured with a BRUKER ultrafleXtreme MALDI-TOF spectrometer. Ultraviolet-visible (UV-vis) absorption spectra were obtained on a Hitachi U-3900 UV–Vis spectrophotometer. PL spectra and phosphorescent spectra were obtained on a Hitachi F-4600 fluorescence spectrophotometer. PL lifetime spectra was obtained on HAMAMATSU compact fluorescence lifetime spectrometer C11637. The photoluminescence quantum yield (PLQY) was measured using HAMAMATSU C9920-02G. Thermogravimetric analysis (TGA) was performed on a TA SDT 2960 instrument at a heating rate of 10 □/min under nitrogen. Differential scanning calorimetry (DSC) was performed on a TA DSC 2010 unit at a heating rate of 10 □ min^{-1} under nitrogen. Cyclic voltammetry (CV) was carried out on a CHI600 voltammetric analyzer at room temperature with ferrocenium-ferrocene (Fc^{+}/Fc) as the internal standard. A conventional three-electrode configuration consisting of a Pt-wire counter electrode, an Ag/AgCl reference electrode, and a platinum working electrode was used. The oxidative scans were performed at a scan rate of 0.05 V s^{-1}. Degassed DCM was used as solvent for oxidation scan with tetrabutylammonium hexafluorophosphate ($TBAPF_6$) (0.1 M) as the supporting electrolyte.

Device fabrication and measurements

The OLED devices were fabricated through vacuum deposition on commercial pre-patterned ITO-coated glass substrates (ITO: 185 nm; Glass: 32 mm×32 mm×0.7 mm) with the sheet resistance of 6 Ω per square under high vacuum of 4×10^{-6} Torr. The active area of each device is 3 mm □ 3 mm. The ITO substrates were cleaned by sonication in acetone, ethanol, and deionized water for 15 min subsequently, and then dried in an oven at 110 °C and treated by UV ozone for 15 min. The deposition rates were controlled at 0.3-0.4 Å s^{-1} for HAT-CN, 0.2-0.4 Å s^{-1} for Liq, 1-2 Å s^{-1} for other organic layers and 6-8 Å s^{-1} for Al anode. The EL spectra, CIE

coordinates, *J–V–L* curves, CE and PE of the devices were measured with a programmable spectra scan photometer (PHOTO RESEARCH, PR 655) and a constant current source meter (KEITHLEY 2400) at room temperature.

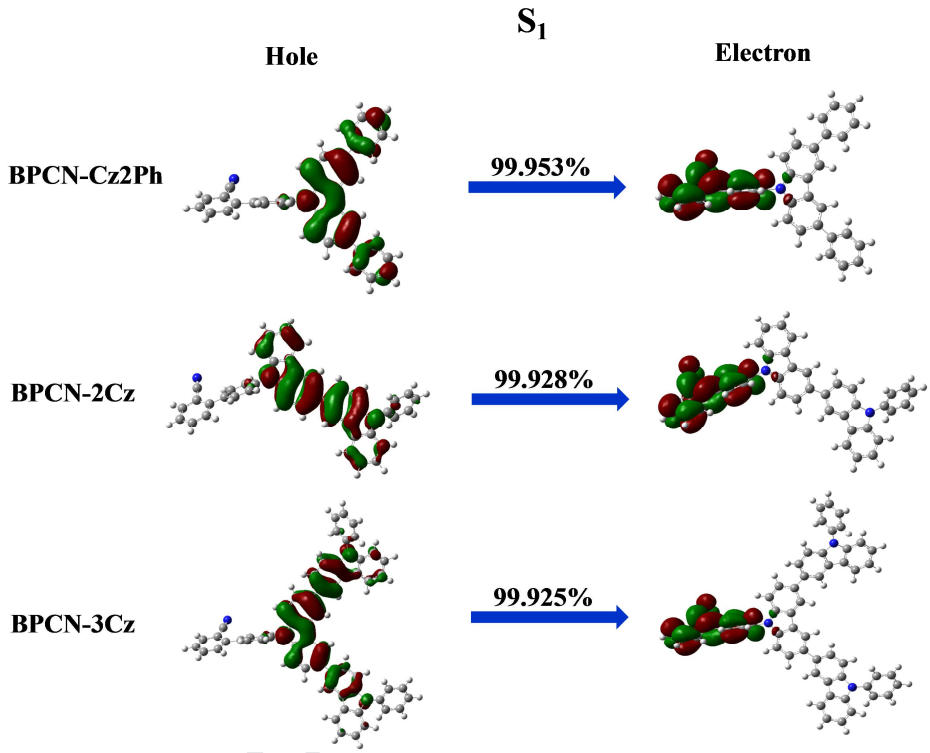

Fig. S1. NTO of singlet states for **BPCN-Cz2Ph**, **BPCN-2Cz** and **BPCN-3Cz**.

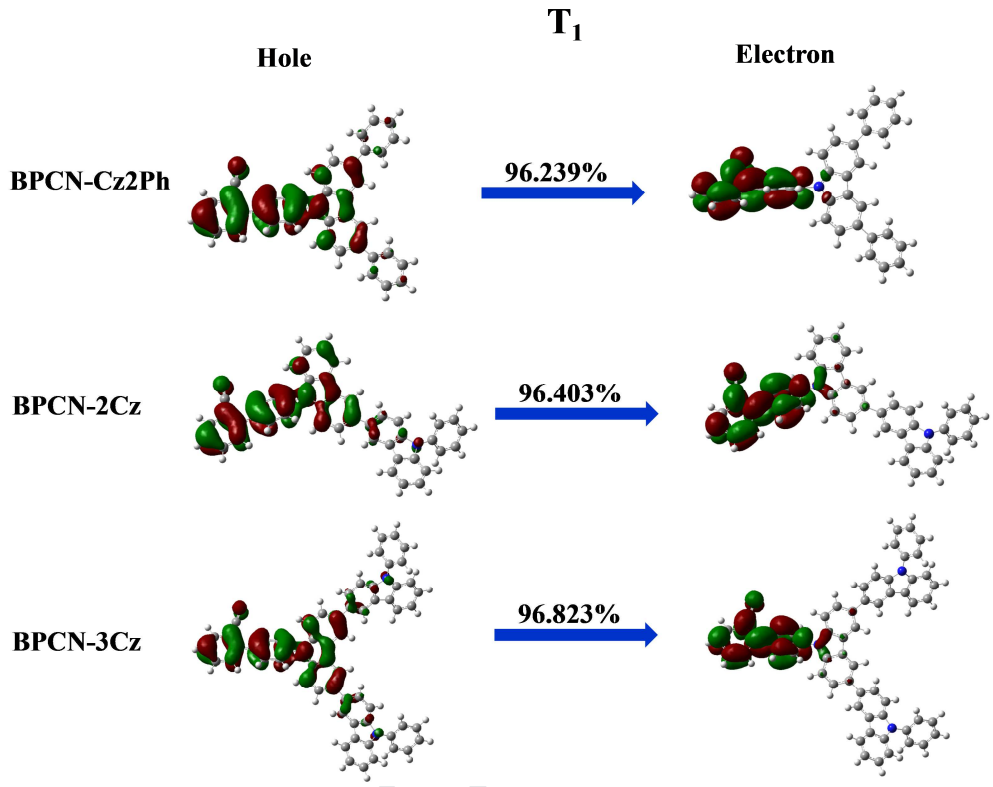

Fig. S2. NTO of triplet states for **BPCN-Cz2Ph**, **BPCN-2Cz** and **BPCN-3Cz**.

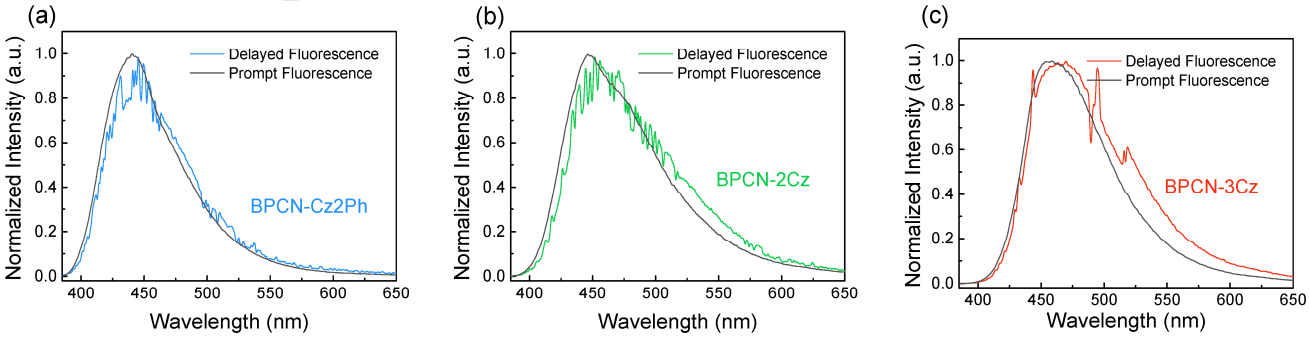

Fig. S3. Delayed and prompt fluorescence spectra of **BPCN-Cz2Ph**, **BPCN-2Cz**, and **BPCN-3Cz**.

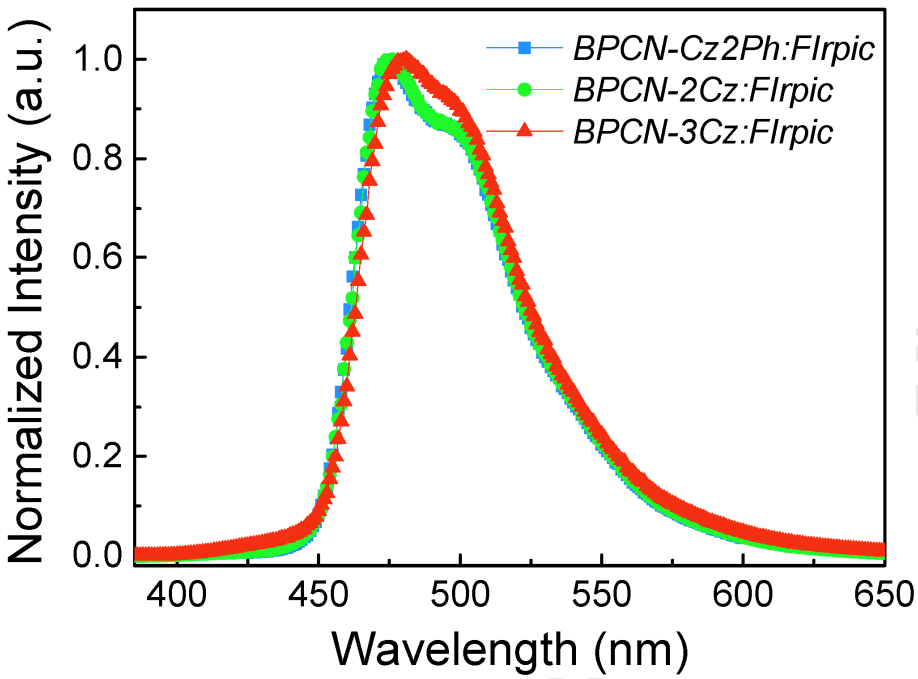

Fig. S4. PL spectra of FIrpic co-deposited with **BPCN-Cz2Ph**, **BPCN-2Cz**, and **BPCN-3Cz**.

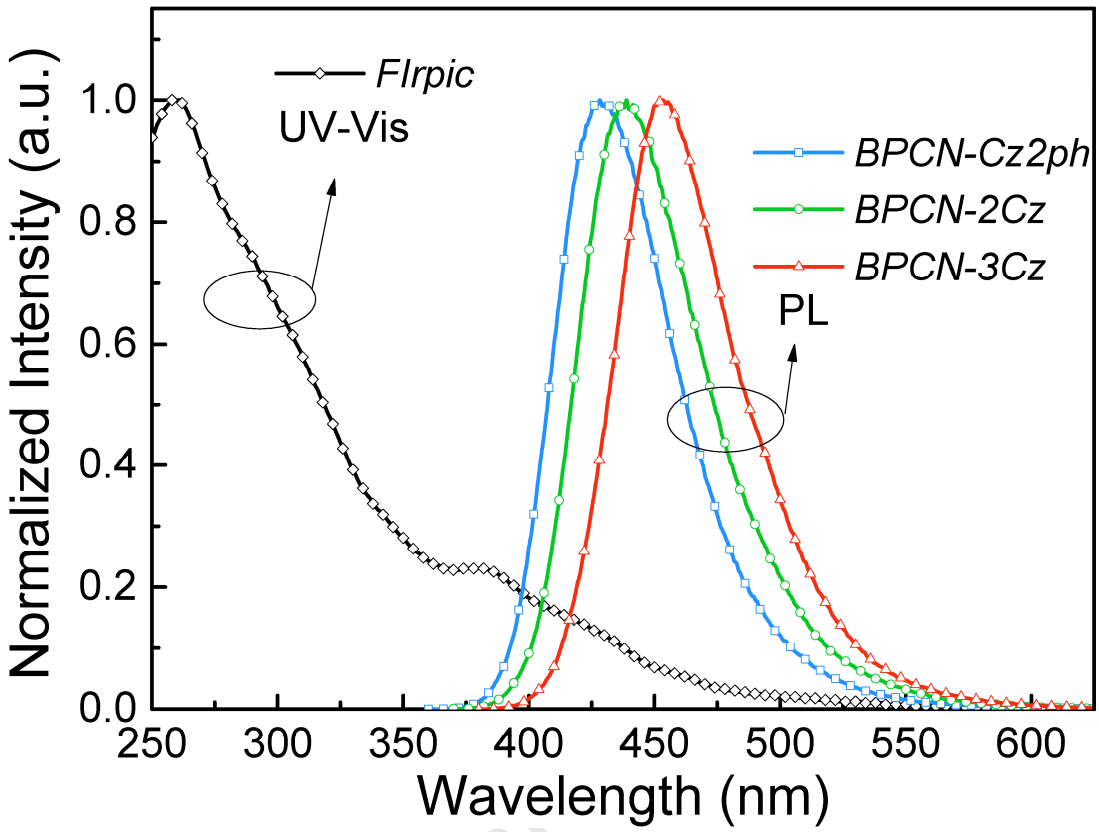

Fig. S5. The absorption spectrum of FIrpic and PL spectra of **BPCN-Cz2Ph**, **BPCN-2Cz**, and **BPCN-3Cz** neat films.

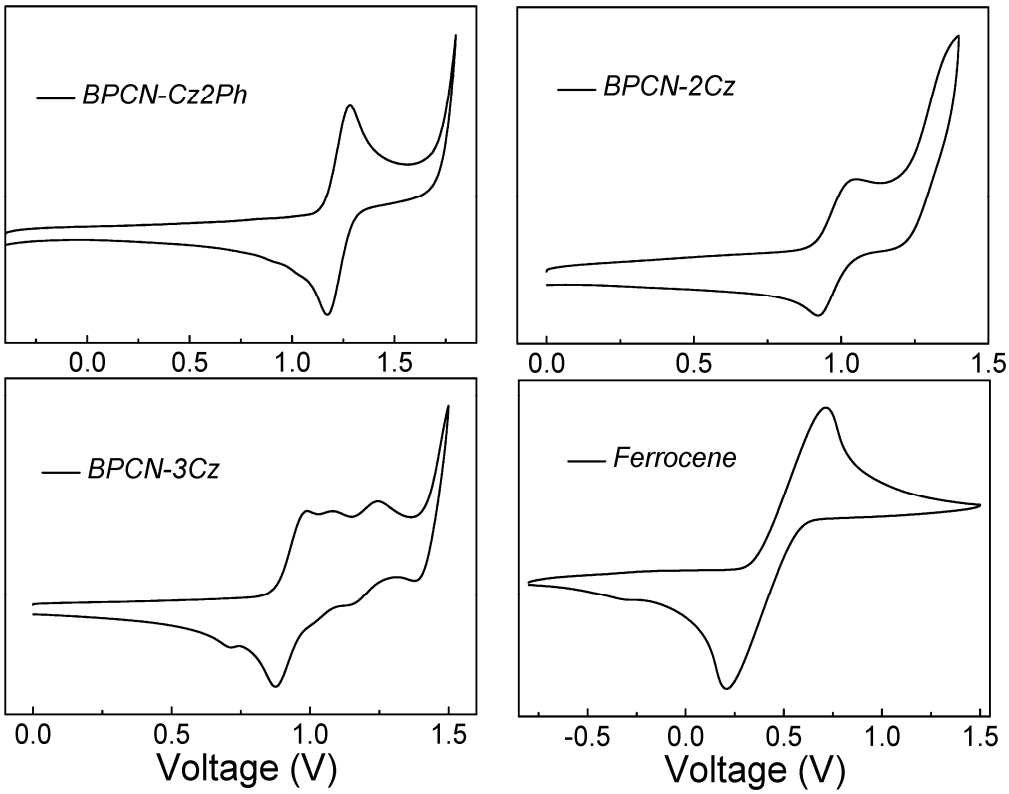

Fig. S6. Cyclic voltammograms of **BPCN-Cz2Ph**, **BPCN-2Cz**, **BPCN-3Cz,** and ferrocene.

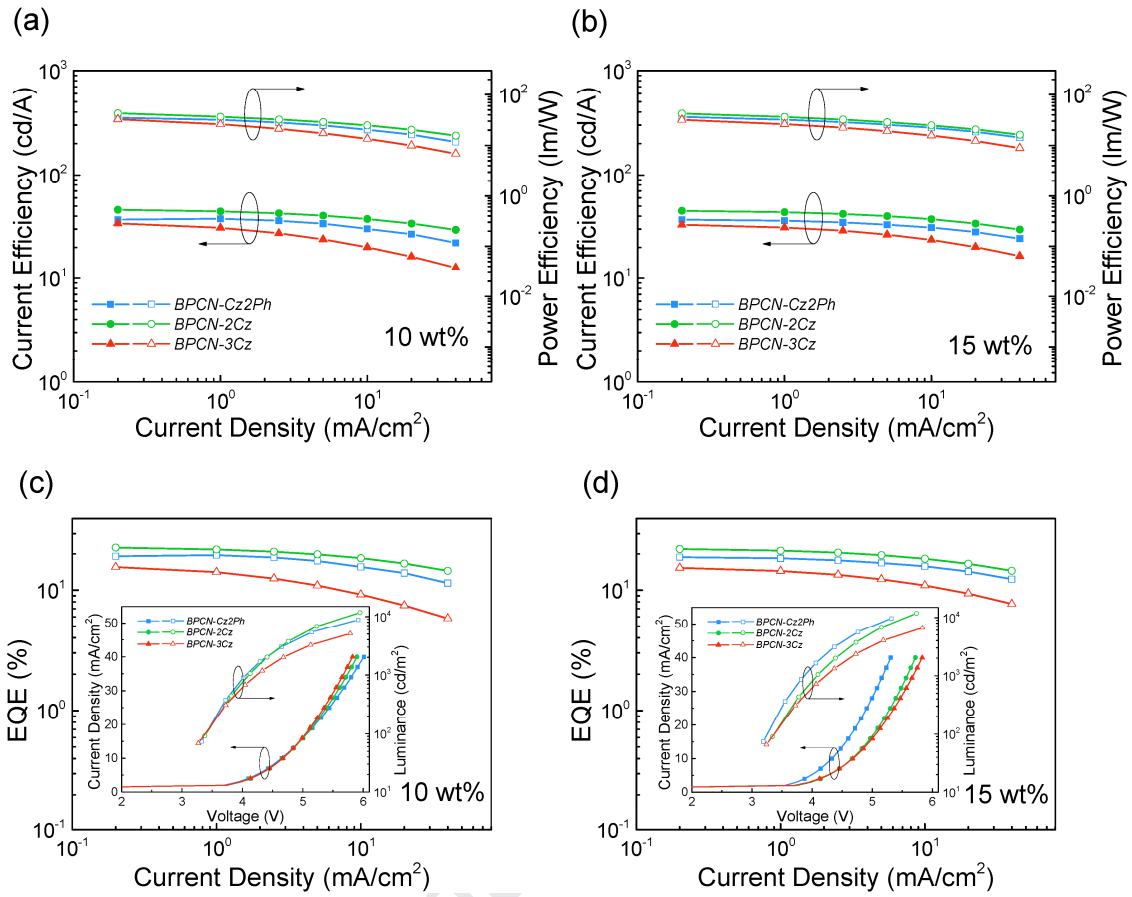

Fig. S7. CE-*J*-PE curves of **BPCN-Cz2Ph**, **BPCN-2Cz**, and **BPCN-3Cz** based devices with doping ratio of (a) 10 wt% and (b) 15 wt%; EQE-*J* curves of **BPCN-Cz2Ph**, **BPCN-2Cz**, and **BPCN-3Cz** based devices with doping ratio of (c) 10 wt% and (d) 15 wt% (inset: *J*-*V*-*L* curves of **BPCN-Cz2Ph**, **BPCN-2Cz**, and **BPCN-3Cz** based devices with doping ratio of 10 wt% and 15 wt%).

Table S1. Photophysical properties of FIrpic co-deposited with **BPCN-Cz2Ph**, **BPCN-2Cz** and **BPCN-3Cz**.

Host	Guest	$\tau^{a)}$ [μs]	$\eta_{PL}{}^{b)}$ [%]	$k_r{}^{c)}$ [10^5 s^{-1}]	$k_{nr}{}^{c)}$ [10^5 s^{-1}]
BPCN-Cz2Ph	FIrpic	1.71	85	4.98	0.88
BPCN-2Cz	FIrpic	1.91	91	4.76	0.47
BPCN-3Cz	FIrpic	1.41	52	3.68	3.39

[a)]τ = phosphorescent lifetime; [b)]η_{PL} = photoluminescence quantum efficiency; [c)]radiative and nonradiative rate constants (k_r and k_{nr}).

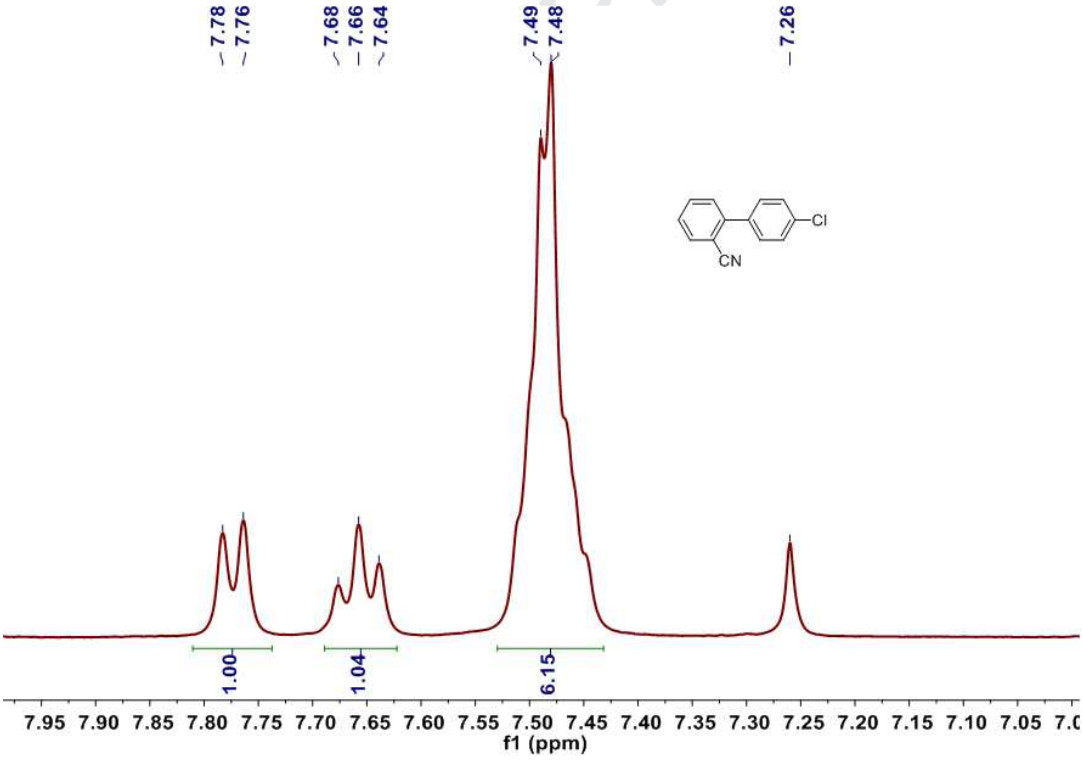

Fig. S8. ^{1}H NMR spectrum of 4'-chloro-[1,1'-biphenyl]-2-carbonitrile (400 MHz, $CDCl_3$).

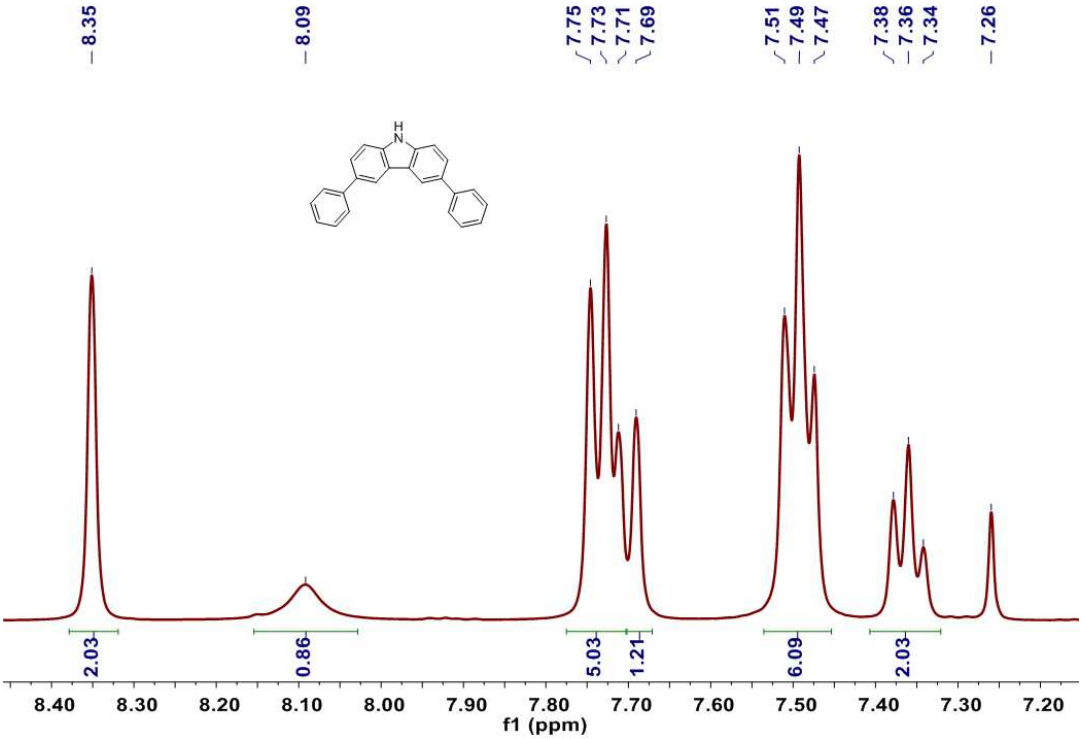

Fig. S9. ^{1}H NMR spectrum of 3,6-diphenyl-9*H*-carbazole (1) (400 MHz, $CDCl_3$).

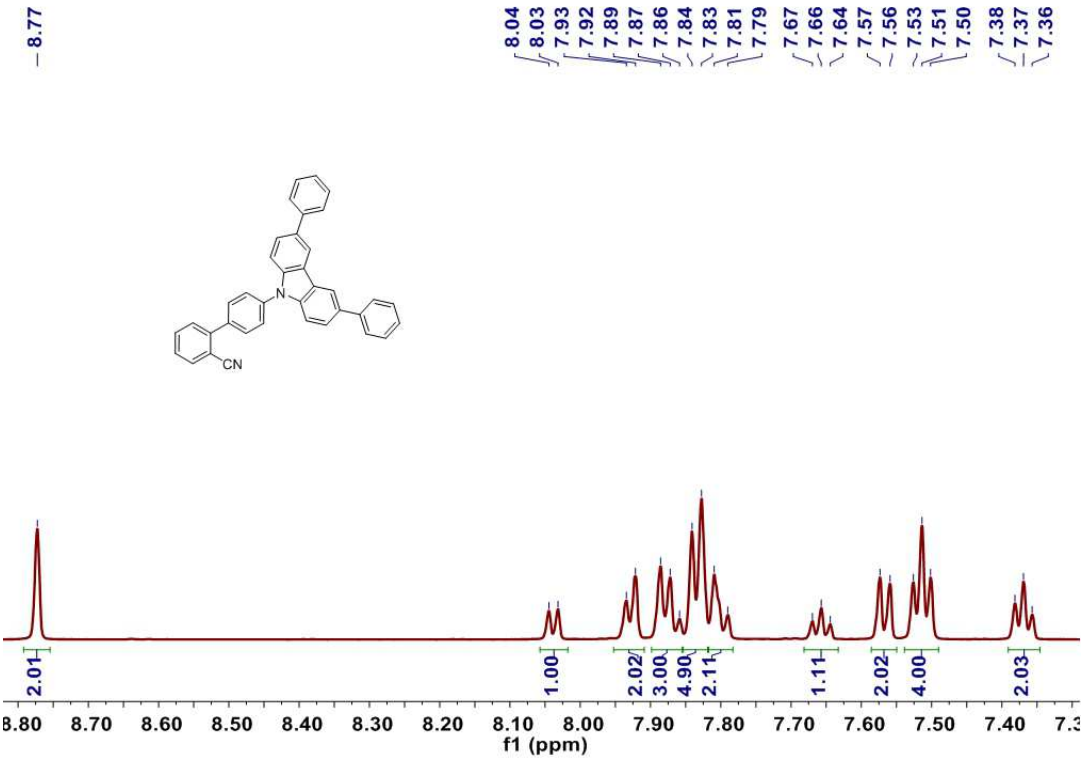

Fig. S10. ^{1}H NMR spectrum of **BPCN-Cz2Ph** (600 MHz, DMSO).

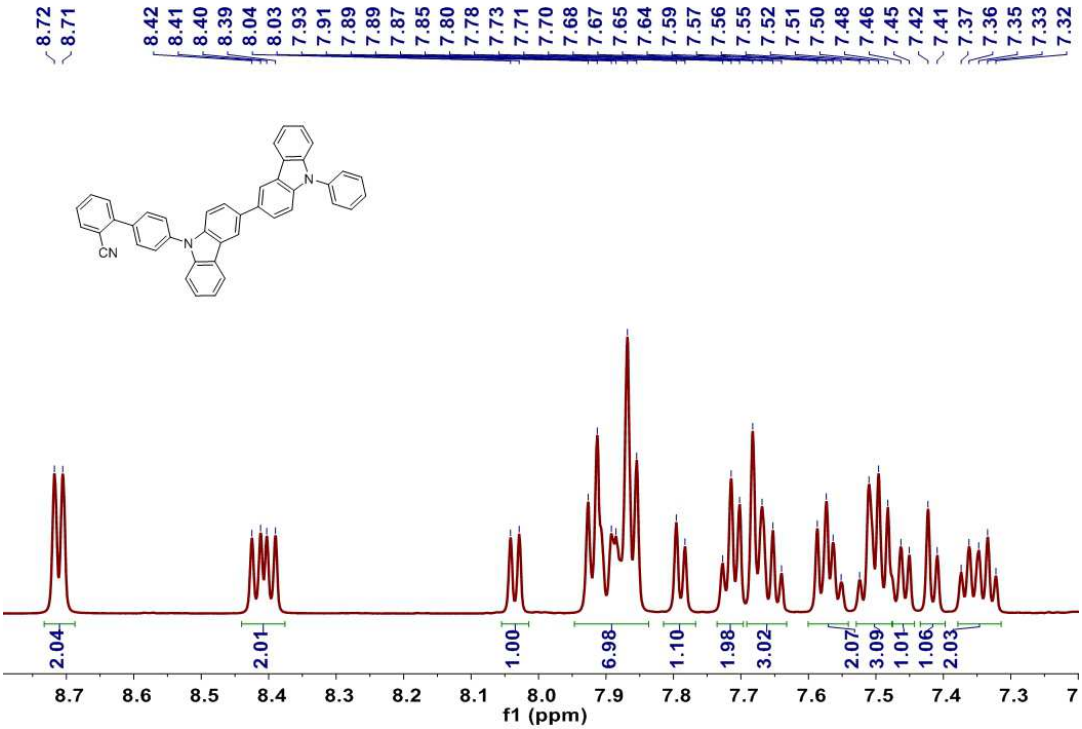

Fig. S11. ^{1}H NMR spectrum of **BPCN-2Cz** (600 MHz, DMSO).

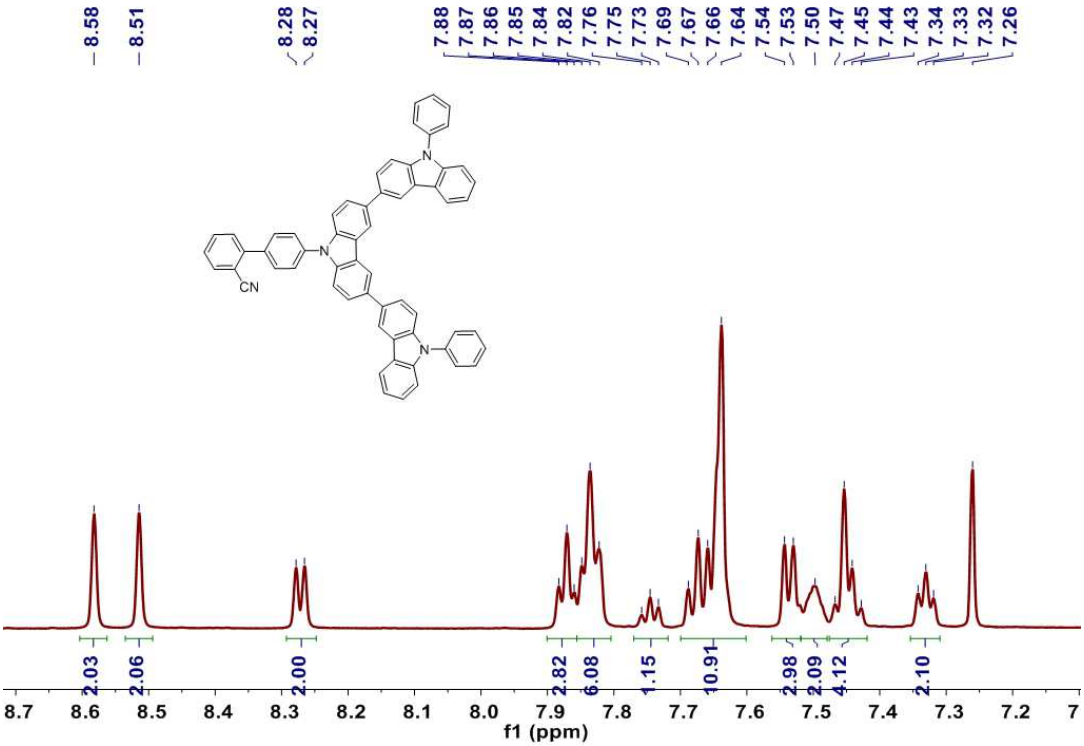

Fig. S12. ^{1}H NMR spectrum of **BPCN-3Cz** (600 MHz, $CDCl_3$).

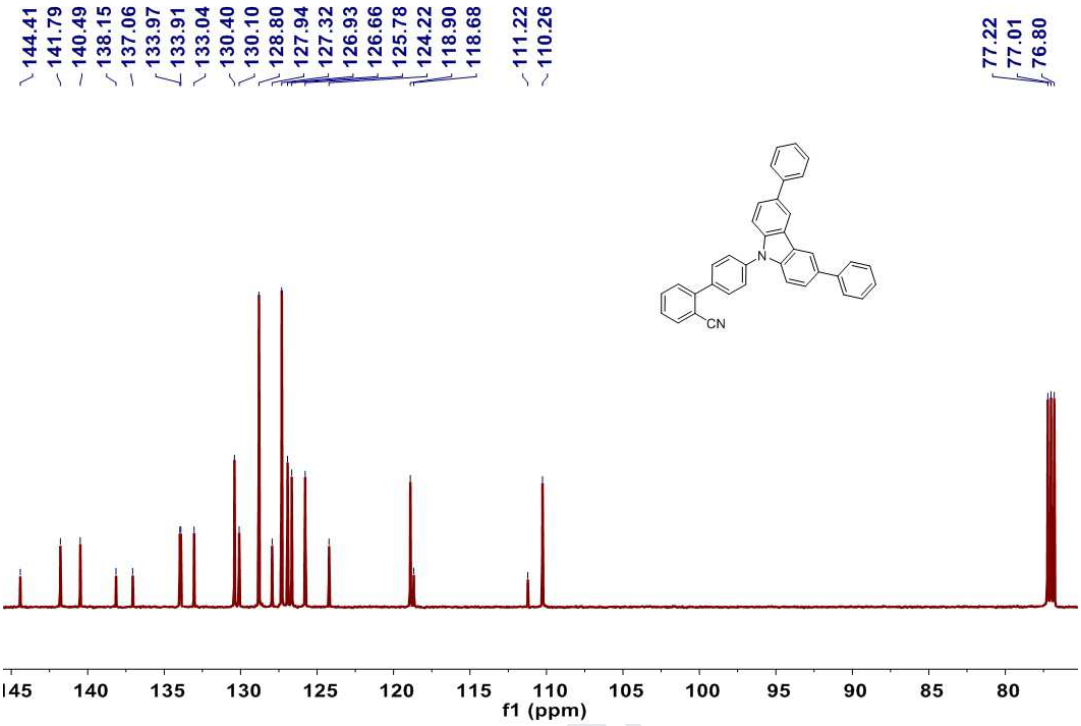

Fig. S13. ^{13}C NMR spectrum of **BPCN-Cz2Ph** (151 MHz, $CDCl_3$).

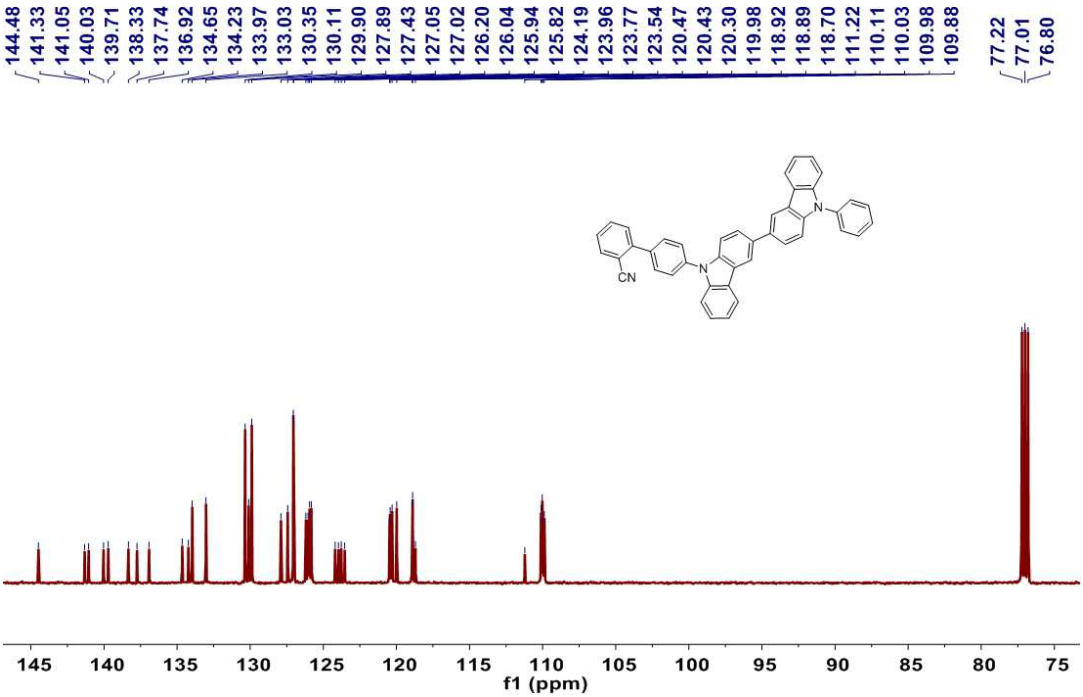

Fig. S14. ^{13}C NMR spectrum of **BPCN-2Cz** (151 MHz, $CDCl_3$).

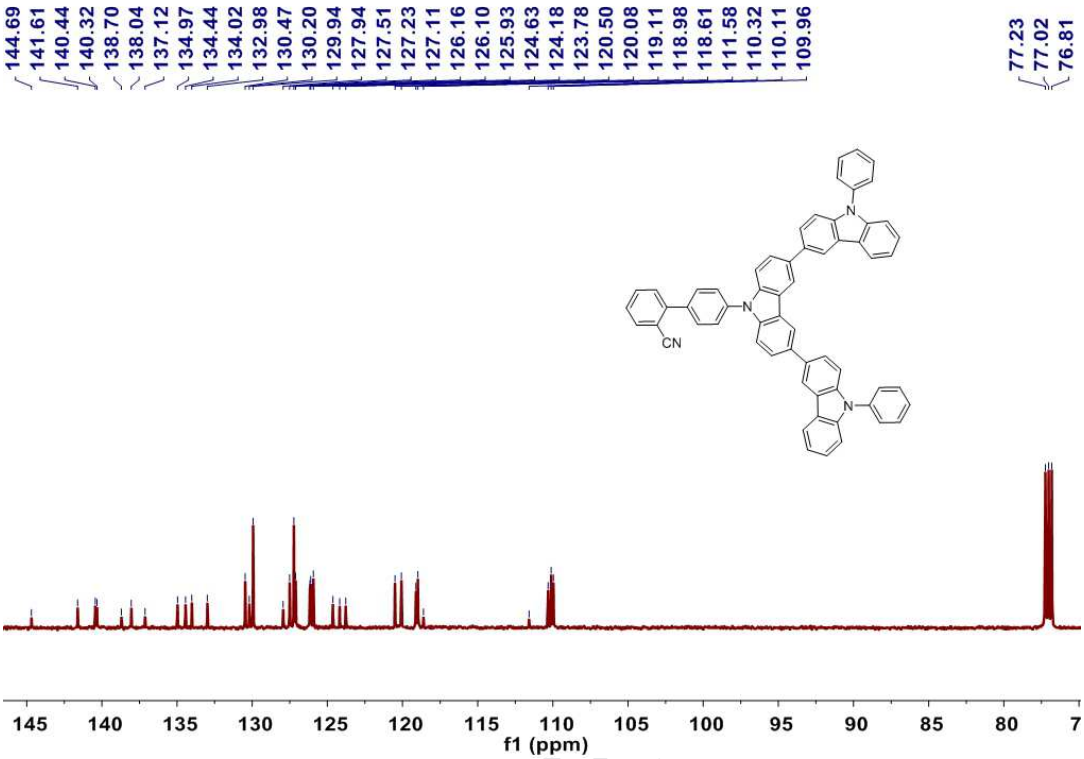

Fig. S15. ^{13}C NMR spectrum of **BPCN-3Cz** (151 MHz, $CDCl_3$).

Highlights:

- Three novel wide-bandgap **TADF** host materials **BPCN-Cz2Ph**, **BPCN-2Cz** and **BPCN-3Cz** are designed and synthesized.
- High efficiency with **CE** of 50.0 cd/A, **PE** of 46.8 lm/W, and **EQE** of 24% is demonstrated in the blue **PHOLEDs** employing **BPCN-2Cz** as the host material.
- Such results indicate an excellent combination of TADF property, high triplet energy, and balanced carrier-transporting ability allow host materials to deliver a high performance.

Declaration of interests

☒ The authors declare that they have no known competing financial interests or personal relationships that could have appeared to influence the work reported in this paper.

☐The authors declare the following financial interests/personal relationships which may be considered as potential competing interests: